Maria João Cunha Coelho Rodrigues Carreiro

Degree in Genetics and Biotechnology

New hepatic cell lines for research, drug testing and vaccine development:

Molecular tools for high-throughput screening of HCV replicating cells

Dissertation to obtain a

Master´s Degree in Biotechnology

Supervisor: Ana Filipa Rodrigues, PhD, iBET & ITQB - NOVA

FACULDADE DE CIÊNCIAS E TECNOLOGIA
UNIVERSIDADE NOVA DE LISBOA

December 2020

Maria João Cunha Coelho Rodrigues Carreiro

Degree in Genetics and Biotechnology

New hepatic cell lines for research, drug testing and vaccine development:

Molecular tools for high-throughput screening of HCV replicating cells

Dissertation to obtain a

Master´s Degree in Biotechnology

Supervisor: Ana Filipa Rodrigues, PhD, iBET & ITQB - NOVA

Jury:

President: Carlos Alberto Gomes Salgueiro, PhD

Arguer: Sandra Cristina de Oliveira Viegas, PhD

December 2020

New hepatic cell lines for research, drug testing and vaccine development

Acknowledgments

Estou eternamente grata por ter chegado fim do mestrado. Quero agradecer a todos os intervenientes que direta ou indiretamente me ajudaram a atingir o meu objetivo.

To Dr. Ana Sofia Coroadinha, for giving me the opportunity to work in the Cell Line Development and Molecular Virology Laboratory and for the great scientific advices and good work environment offered.

A special acknowledgement to my supervisor Dr. Ana Filipa Rodrigues for everything, all the support, scientific guidance, and inspiration to be better and achieve great things. Thank you for allowing me to do mistakes and learn from them.

To all CLD&MV group, Ana Isabel, Miguel, Sofia, Ana Oliveira, Tiago, Maria, Rodrigo, Mariana, Elisa and Catarina for all the help, support and guidance given throughout this year. A very special thanks goes to my beloved Raquel and Joana for the laughs, tears and advices shared, and for being my daily mental and emotional support.

A todos os meus amigos, pelo apoio e ânimo que deram ao longo do mestrado, sem os quais não chegava ao fim deste ano com sanidade mental.

À minha família, a quem tudo devo, que sempre tiveram do meu lado e com a maior paciência para me aturar. Um obrigado especial aos meus irmãos, que mesmo não sabendo, me fazem tornar melhor.

Abstract

Hepatitis C virus (HCV) is a main contributor to chronic liver disease, causing a major social and economic burden worldwide. There is a demand for the development of a vaccine to prevent transmission and eliminate HCV infection. This development has been limited by the lack of research and improved tools, including *in vitro* hepatic cell model permissive to HCV wild-type infection.

This work aimed at developing and validating the molecular tools for a high-throughput screening of highly competent hepatic cell lines in supporting the HCV life-cycle, and implementing and optimizing protocols to produce and handle HCV. This molecular tool consisted of a full-length replicon based on the J6/C tagged with a GFP reporter, enabling to identify HCV permissive cells. Since the tagged replicon consists of a RNA molecule, we started by optimizing method for delivering into Huh-7.5 cells, using Lipofectamine MessengerMAX, and by implementing an *in vitro* transcription (IVT) protocol. Additionally, we establish reporter plasmids to produce control transcripts, suiting the purpose of IVT validation and to function as a transfection internal control. As a mechanism for translation initiation in these reporter constructions, two possibilities were evaluated: a cap-dependent mechanism, using ARCA, and a cap-independent mechanism, based on four types of IRES. After establishing the protocols to produce and deliver the tagged replicon into cells, the functionality of this RNA construction was confirmed by the reporter gene expression, when transfected in Huh-7.5 cell line. After the validation of the reporter capacity of the tagged replicon, to continuo in the follow-up of this thesis, new hepatic cell lines established by immortalization from primary human hepatocytes will be assessed their ability to support the HCV life cycle.

This work contributed to create a methodology for screening improved hepatic cell lines to better serve research, drug testing and vaccine development against HCV.

Keywords: HCV; Tagged replicon; Lipofection; *In vitro* transcription; human hepatic cell lines.

Resumo

O vírus da hepatite C (HCV) é a maior causa da doença hepática crónica, tendo um grande impacto social e económico a nível mundial. Existe um grande investimento no sentido de desenvolver uma vacina contra o HCV, prevenir a sua transmissão e eliminar a infeção causada pelo vírus. No entanto, o desenvolvimento de vacinas está limitado pela falta de boas ferramentas de investigação, como modelos celulares hepáticos *in vitro* que sejam permissivos à infeção pelo HCV *wild-type*.

Este trabalho teve como objetivo o desenvolvimento e a validação de uma ferramenta molecular, permitindo selecionar rapidamente linhas células hepáticas competentes e capazes de suportar o ciclo de vida do HCV e implementar os protocolos otimizados necessários para produzir e manipular o vírus. Esta ferramenta molecular consiste no replicão completo J6/C marcado com o repórter GFP, permitindo selecionar células permissivas ao vírus. Dado que este replicão marcado consiste numa molécula de RNA, começámos por otimizar o método de entrega das moléculas à linha celular Huh-7.5, usando lipofectamina MessengerMAX e por implementar um protocolo de transcrição *in vitro* (IVT). Estabelecemos um plasmídeo repórter para produzir os transcritos de controlo, permitindo a validação da IVT, e funcionar como controlo interno de transfeção. Como mecanismo de iniciação de tradução deste transcrito, foram testados: o mecanismo dependente de cap, usando a ARCA, e o mecanismo independente de cap, testando quarto tipos de IRES. Após estabelecidos os protocolos para produzir e entregar o replicão marcado às células, foi confirmada a sua funcionalidade através da expressão do gene repórter. Depois de validar a capacidade repórter do replicão marcado, no seguimento desta tese, novas linhas celulares hepáticas estabelecidas por imortalização de hepatócitos humanos primários serão avaliadas na capacidade de suportar o ciclo de vida do HCV.

Este trabalho contribuiu para o desenvolvimento de uma metodologia de seleção de linhas celulares hepáticas melhoradas, permitindo o estudo do HCV, o teste de novos fármacos e o desenvolvimento de uma vacina contra o HCV.

Palavras-chave: HCV; Replicão marcado com GFP; Lipofeção; Transcrição *in vitro*; linha celular hepática humana.

List of Contents

List of Figures

List of Tables

List of Abbreviations

5xRRL	5x Rabbit reticulocyte lysate equivalent buffer
ATCC	American Type Culture Collection
Av	Average
C	Core protein
cDNA	Complementary deoxyribonucleic acid
CLDN	Claudin
CO2	Carbon dioxide
CV	Coefficient of variation
DAAs	Direct-acting antivirals
DMEM	Dulbecco's Modified Eagle's Medium
DMSO	Dimethyl sulfoxide
DNA	Deoxyribonucleic acid
DNA	Desoxyribonucleic acid
DNAse	Desoxyribonuclease
E1	Envelope glycoprotein 1
E2	Envelope glycoprotein 2
eGFP	Enhanced green fluorescent protein
eIF	eukaryotic initiation factor
EMCV	Encephalomyocarditis virus
FBS	Fetal bovine serum
FC	Flow cytometry
GFP	Green fluorescent protein
GT	Genotype
HAV	Hepatitis A virus
HCV	Hepatitis C Virus
HCVwt	Hepatitis C virus wild type
HEK	Human embryonic kidney
HIV-1	Human immunodeficiency virus-1
IRES	Internal ribosome entry site
ITAF	IRES *trans*-acting factors
IVT	*In vitro* transcription
JFH1	Japanese fulminant hepatitis strain

kb	Kilobase pairs
LF	Lipofectamine
MCS	Multiple cloning site
mRNA	Messenger RNA
NEB	New England Biolabs
NS	Non-structural
ORF	Open reading frame
PCR	Polymerase chain reaction
PEI	Polyethylenimine
PHH	Primary human hepatocytes
PV	Polio virus
rATP	Ribonucleoside adenosine triphosphates
rCTP	Ribonucleoside cytosine triphosphates
RdRp	RNA-dependent RNA polymerase
REMs	Replication enhancing mutations
rGTP	Ribonucleoside guanosine triphosphates
RNA	Ribonucleic acid
RNAse	Ribonuclease
rNTPs	Ribonucleotide triphosphates
RT-qPCR	Real-time quantitative PCR
rUTP	Ribonucleoside uracil triphosphates
siRNA	Small interfering RNA
SV40	Simian vacuolating virus 40
TERT	Telomerase reverse transcriptase
UTR	Untranslated region
WHO	World Health Organization

1. INTRODUCTION

1.1. Hepatic infections

The liver is the largest internal organ in humans and it is responsible for more than 500 functions comprising metabolic, synthetic, immunologic and detoxification processes[1–5]. It presents a multicellular architecture in a highly complex *in vivo* microenvironment, where hepatocytes represent two-thirds of liver cell mass[1]. These cells are targeted by several hepatotropic pathogens, such as viruses, bacteria and parasites to complete their life cycle or for development stages[5].

Among hepatotropic pathogens, the hepatitis C virus (HCV) represents a major social and economic burden. Around 71 million people are affected by HCV worldwide and, every year, 1.75 million new infections arise[6]. HCV is the main contributor to chronic liver disease, causing chronic hepatitis, hepatocellular carcinoma and liver cirrhosis[7–9]. Ultimately, HCV can lead to an increased morbidity and mortality in more than 70% of infected people[7,8], which reflects on approximately 400 000 deaths per year[7,10]. By the year of 2030, the Global Health Sector Strategy intends to eliminate hepatitis infection through an increase of screening and treatment, and by reinforcing prevention[11]. Moreover, the World Health Organization (WHO) aims to reduce 90% of newly infected individuals, to reduce 65% of infection-related deaths, and to treat 80% of patient suffering with chronic hepatitis C until 2030[7].

Currently there are available treatments for HCV infection, being direct-acting antivirals (DAAs) the most efficient. DAAs target HCV specific nonstructural viral proteins, such as the proteases, which play a crucial role in the HCV life cycle[12]. DAAs achieve high rates of sustained virological responses for most HCV genotypes[7,13], in a short period of treatment and presents few side effects[13]. They also deliver a better clinical outcome than previous interferon-based and ribavirin treatments[14]. Although these drugs are highly effective, the drug pricing is still a problem to reach the treatment in many sub-developed counties[11] and induces the mechanism of resistance that reduces drug activity[15,16].

The development of a vaccine is crucial for an effective elimination of HCV infection and to reduce HCV prevalence and propagation, which is essential to achieve the WHO goal of eliminating HCV by the year of 2030 and reduce the burden caused by HCV worldwide[17]. This development has been limited by the lack of research and development tools, including robust and reliable hepatic culture systems for the study of HCV, and for developing and validating new therapeutic and prophylactic solutions against the virus[18,19].

1.2. Hepatitis C virus biology

Hepatitis C virus is a single stranded RNA (ssRNA) enveloped virus, belonging to the *Hepacivirus* genus of the *Flaviviridae* family[8–10,20]. This virus presents a wide genetic heterogeneity being classified into

7 major genotypes and numerous subgenotypes based on phylogenetic and sequence analyses[8,10,21]. This variety of genotypes can be explained by the viral RNA polymerase which lacks proof-reading activity and causes a high mutation rate in the viral genome[22]. The distribution of genotypes is different around the globe being genotypes 1 and 3 the most prevalent. This high heterogeneity has a significant impact on clinical pathologies, disease severity, antiviral drug response, and even on the development of an effective vaccine due to distinct behavior of the different genotypes[9,10,18,23].

HCV genome is a 9.6 kb length positive ssRNA molecule with only one open reading frame (ORF) encoding a polyprotein of about 3000 amino acids, flanked by complex RNA structures, the untranslated regions (5'UTR and 3´UTR) (Figure 1.1). The 5´UTR functions as an internal ribosome entry site (IRES) and 3´UTR is essential for replication[10,24–26]. The polyprotein is produced in association with the endoplasmic reticulum, and processed and cleaved at the co- and post-translation level by host and viral proteases[9]. This gives rise to three structural proteins (the core (C) and envelope glycoproteins E1 and E2) and seven nonstructural proteins which are responsible for processing, replication and viral assembly (p7, NS2, NS3, NS4A, NS4B, NS5A and NS5B)[9,10,25].

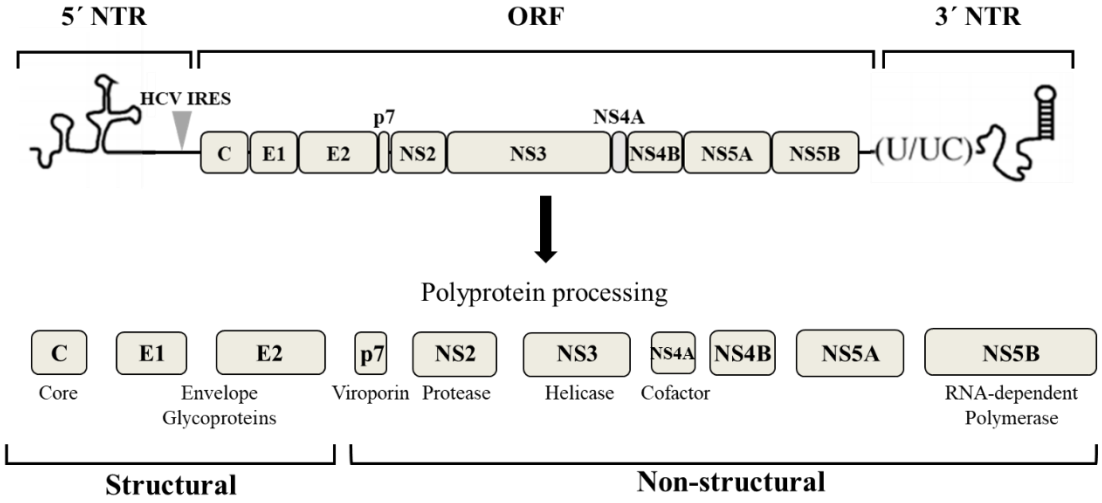

Figure 1.1 - Hepatitis C virus genome and derived proteins. NTR: non-translated region; ORF: open reading frame.

The core protein has a structural function, which allows the viral capsid formation and protects the viral genome[27,28]. E1 and E2 are the envelope glycoproteins involved in viral assembly, HCV attachment and entry into host cell and endosomal membrane fusion. Nonstructural protein p7 is a small transmembrane viroporin essential for HCV assembly and release from the host cells[29]. NS2 function as a viral protease participating in the maturation of the polyprotein and as cofactor in the viral assembly[13,25,30,31]. NS3 is a bifunctional enzyme, functioning as a viral protease and, when associated with its co-factor, NS4A[13], also works as a complex with RNA helicase activity[25,32,33]. This helicase activity has an important role in

separating RNA complex structures allowing proteins displacement along the RNA[9]. NS4B is responsible for the replication complex formation and alterations in the cell membrane for virus-host interactions for host signal transduction pathways[34–36], while NS5A phosphoprotein is involved in replication regulation and in virus assembly, when associated with several host and viral proteins[37]. NS5B is a RNA-dependent RNA polymerase (RdRp) which belongs to HCV replicase complex[9,25]. During the HCV life cycle, proteins may acquire various structural conformations or establish different interactions with viral or host molecules, resulting into different functionalities[25].

The life cycle of HCV is represented in Figure 1.2. The virus enters the host cell by binding sequentially E1 and E2 glycoproteins to specific membrane receptors, such as SR-BI and CD81. HCV moves laterally through the hepatocyte tight junction and interacts with CLDN1 and OCLN, followed by fusion and endosomes formation[9,13,22,38,39]. In the endosome, the acidic pH causes the fusion the virus and the endosome membranes leading to the disruption of the viral capsid. When the virus is uncoated, its RNA genome is released into cytoplasm[39,40]. The incoming viral RNA is translated by the ribosome into the HCV polyprotein. In endoplasmic reticulum, the polyprotein is processed and cleaved, resulting in ten mature viral proteins[13,41]. Additionally, the viral genome is used as template for replication, carried out by the NS4B-NS5A complex, through the synthesis of an intermediate of (-)-ssRNA[9,13,24]. The newly synthesized (+)-ssRNA is used for translation, replication and for nucleocapsid particle formation[42–44]. Viral assembly is not fully understood, but it is known to occur next to endoplasmic reticulum membranes, where there is a coordinate recruitment, assembly and binding of all viral factors involved in virion formation[13]. The core protein joins the viral genome for nucleocapsid formation and gets surrounded by a lipidic bilayer envelope derived from the membrane of endoplasmic reticulum, producing the infectious virion[9,10]. Then the maturation of the lipoviroparticles occurs, which are composed by triglycerides and apolipoproteins surrounding the envelope glycoproteins[45,46], taking place in the Golgi complex[13]. Finally, HCV particles are released through the fusion of endosomal sorting complexes required for transportation (ESCRTs) with the hepatocyte cell membrane [47–49].

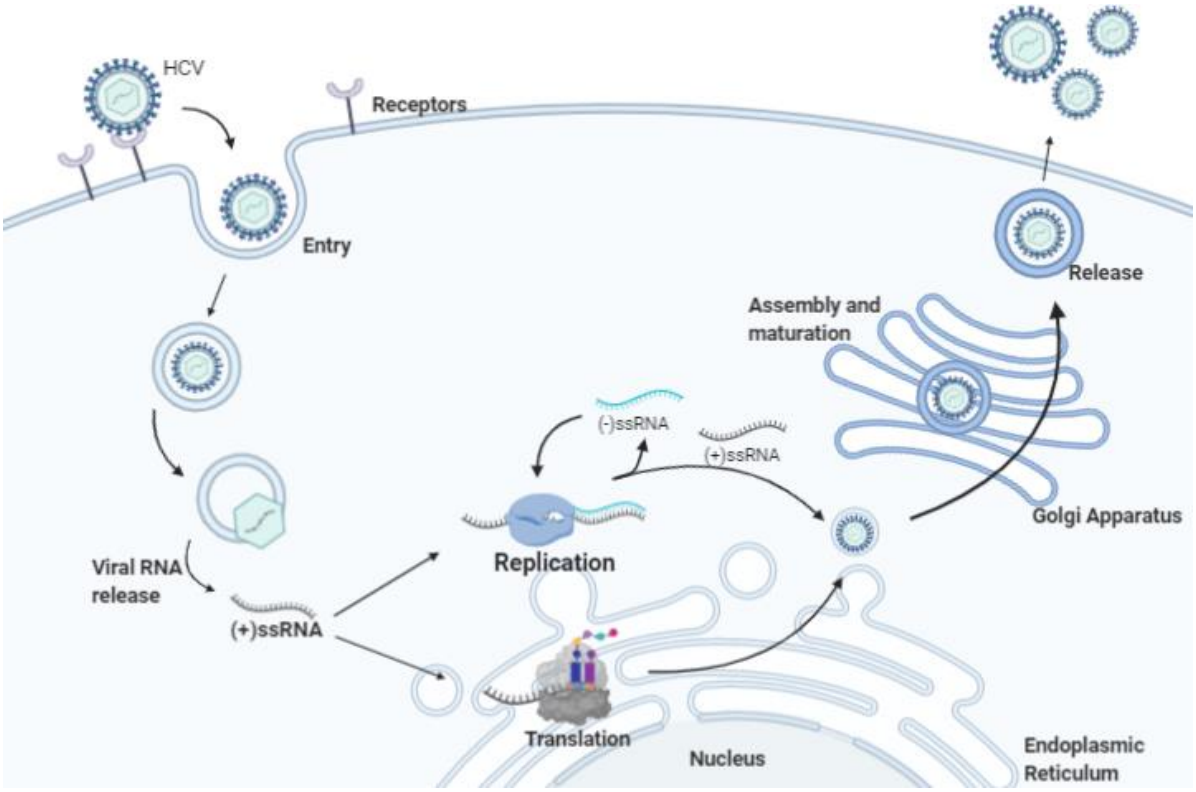

Figure 1.2 - Schematic representation of the HCV life cycle. Adapted from [50]. Figure created with BioRender.com.

1.3. Hepatic cell models

The lack of suitable cell culture systems and animal models that mimic the natural conditions of the liver in humans has been a major limitation in studying HCV[8,9,22,23,51]. The high specificity of the virus for the physiology and metabolism of a mature hepatocytes, makes the use of alternative host cell largely useless[8,52,53].

Primary human hepatocytes (PHH) are considered the best *in vitro* cell model for viral hepatitis studies, liver physiology and regeneration[54], as well as for pharmacological and toxicological research[23,55]. PHH exhibit the metabolism and functionality closely resembling those of mature hepatocytes in the human liver[56], being physiologically relevant and the most suitable cell culture systems for HCV studies[23]. Moreover, *in vitro* cultured PHH are permissive to HCV-positive sera infection, supporting virus replication for two weeks[57], a feature that is not shared by any other cell culture system. The main limitations to PHH use are the low availability, high donor variability, rapid dedifferentiation and low *in vitro* proliferation[23,52,54,58–60]. To overcome this problem, immortalized hepatocytes have been generated using a combination of immortalization genes, such as cellular and viral oncogenes, that are implicated in stimulation of cell cycle progression or in inactivation of cell cycle arrest, and also using the human telomerase reverse transcriptase (hTERT) (reviewed by Ramboer *et al.* [60]). However, immortalization alone

does not guarantee the maintenance of the primary-line features. Additionally, it often results in high clonal variability in cell physiology and metabolism.

Alternative to PHH, human hepatoma-derived cell lines, such as the Huh-7 and their derivatives, are frequently used for HCV studies due to their ability to propagate HCV replicons and to support the assembly of viral particles[61]. Cell lines are readily available and offer unlimited growth, easy handling and high reproducibility[58]. In the case of Huh-7 derivatives, such as Huh-7.5, Huh-7.5.1 and Huh-7-Lunet, they were isolated from the Huh-7 population by a selection process that enabled selecting clones more permissive and effective in supporting HCV replication[52]. Despite their widespread use, these cell lines do not fully mimic the functions and physiological characteristic of a mature PHH[61,62], since they are non-differentiated, poorly polarized and lack some of the mature hepatocyte markers[52]. These missing features, for example the expression of specific cell surface receptors and other liver-specific factors, such as microRNA 122, cholesterol and fatty acid biosynthesis[9], are crucial to support a complete HCV life cycle[8,52].

1.4. Replicon systems for HCV

Viral replicons are widely used to study RNA viruses. These are RNA or DNA molecules derived from a viral genome, that when present intracellularly, are capable of self-replication[63–65]. In the case of HCV, the replicon system emerged in response to the difficulty of studying the virus life cycle, since propagation from patient sera could not be efficiently achieved *in vitro*[10,18,23,52]. Viral replicons can be divided into full-length replicons, containing the complete viral genome, or subgenomic replicons containing only part of the viral genome, established by deleting some or all of the structural proteins[65], which prevents the formation of viral particles (Figure 1.3 A). Sub-genomic replicons are suitable solely for monitoring RNA replication and translation[23,24,52,66]. On the contrary, full-length replicons enable the production of infectious cell cultured-derived (Figure 1.3 B).

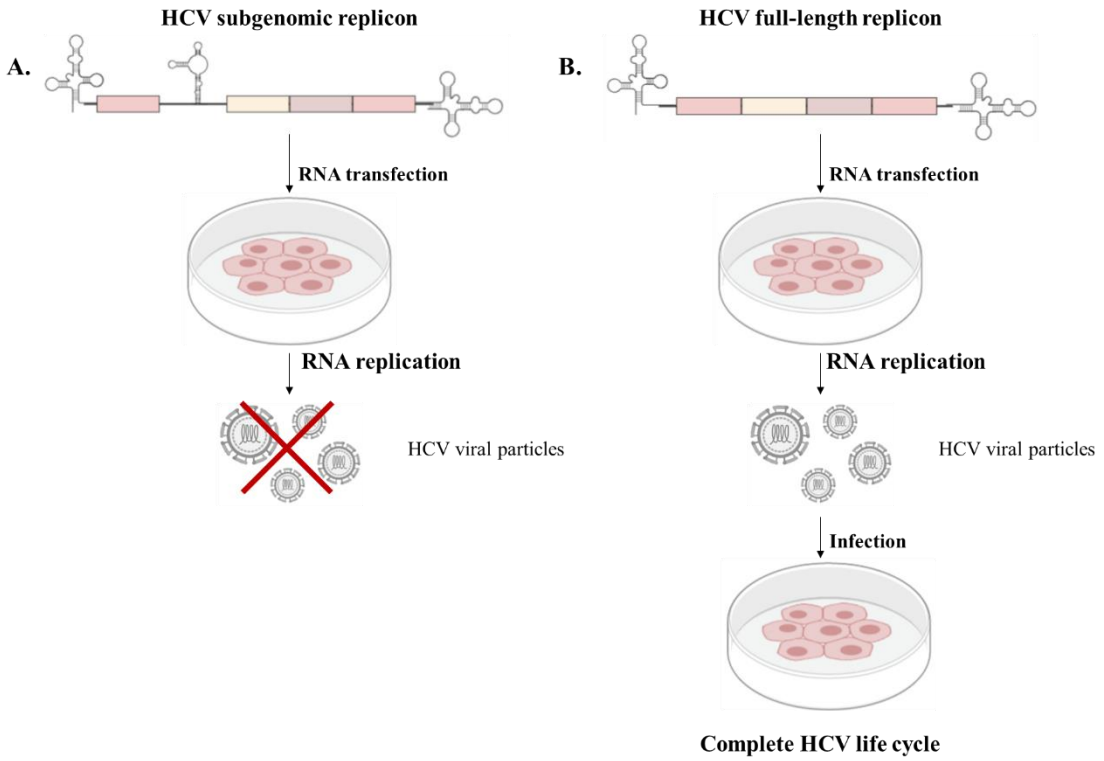

Figure 1.3 – RNA replication and production of cell culture particles with replicons- example for HCV. When HCV subgenomic replicons are transfected into permissive cells, only RNA replication occurs (A). On the other hand, when HCV full-length replicons enable the generation of viral particles named HCVcc (cell culture derived), that are potentially infectious, and can start a new infection (B). Figure created with BioRender.com.

In 1999, the development of the first HCV subgenomic replicon by Lohman *et al.* [24] represented a breakthrough in the field. This replicon consisted of a bicistronic construct containing a heterologous dominant selectable marker - neomycin phosphotransferase (*neo*) gene - under the control of the HCV IRES and the non-structural HCV genes NS3 to NS5B, from genotype 1b, under the control of the encephalomyocarditis virus (EMCV) IRES (Figure 1.4 A). In 2000, this replicon system was expanded to genotype 1a (GT1a) (Figure 1.4 B)[67].

The replication efficiency of subgenomic replicons were low. Also, HCV replicons maintained *in vitro* culture tended to develop replication enhancing mutations (REMs) in the non-structural proteins. These REMs allowed increasing replication yields but were not commonly found in the wild type HCV (HCVwt). Additionally, when applied to full-length replicons these mutations increased the replication efficiency but interfered with the production of infectious particles[52]. In 2003, another subgenomic replicon was developed based on the genome of GT2a isolated from a Japanese patient with "Japanese fulminant hepatitis 1" (JFH1)[66,68] (Figure 1.4 C). This subgenomic replicon presented a major advantage given that it enable a high rate of replication without the accumulation of REMs[18,20,52]. In 2005, a full-length replicon based on JFH1 enable the production of HCVcc particles that were, for the first time, infectious in chimpanzees and PHH[66].

Later, the replicon J6 was created, also derived from GT2a, which could replicate and produce infectious HCVcc (Figure 1.4 D)[23,69]. However, this replicon could not replicate efficiently in cell culture[20].

Although the full-length replicons developed until 2005 represent major achievements for HCV research, they were not representative of all genotypes[18]. In 2006, Pietschmann and colleagues pioneered the establishment of chimeric full-length replicons (Figure 1.4 E), by fusing replication-associated genes (NS3 to NS5B) from JFH1 with the assembly module genes (Core to NS2), from heterologous strains of all major genotypes[52,70]. These chimeric replicons allowed the production of HCVcc harboring the structural proteins from all genotypes.

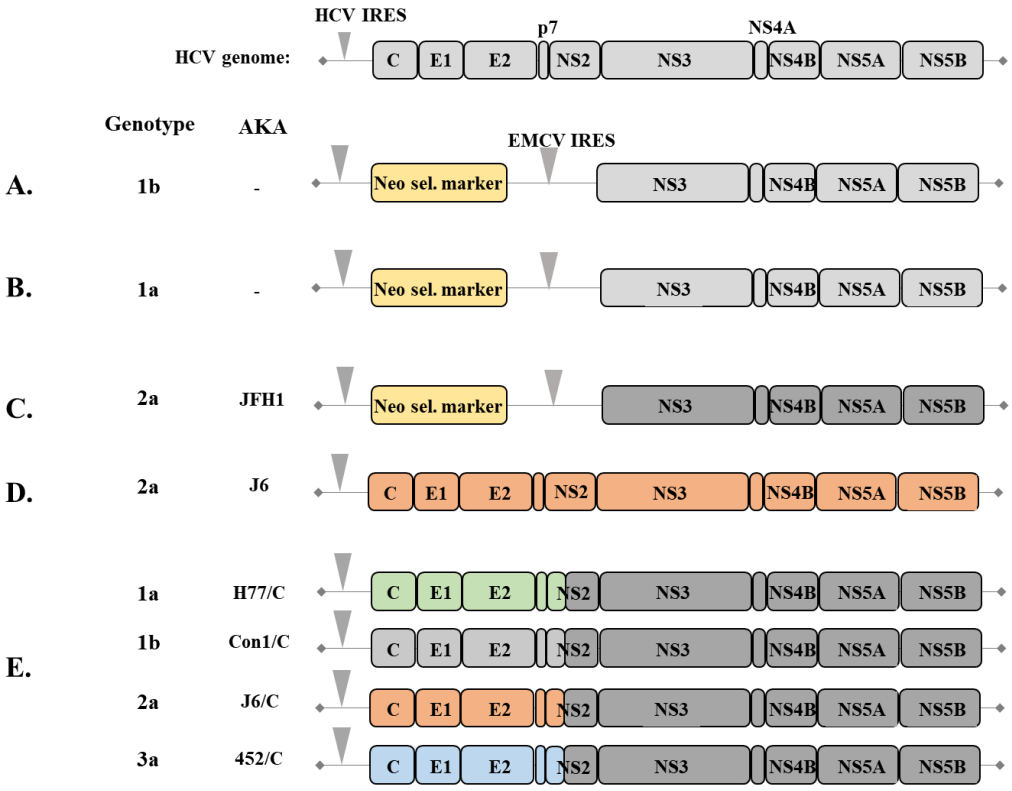

Figure 1.4 - Major historical milestones of HCV replicons. The first replicon system derives from GT1b and it is a bicistronic replicon carrying a selection marker for neomycin and the replication module[24] (A). Replicon system derived from the GT1a, whose constitution is similar to that of GT1b[67] (B). Bicistronic replicon JFH1 with a selection marker[68] (C). Monocistronic full-length replicon derived from GT2a, J6[69] (D). Chimeric replicons resulting from fusing the replication genes from JFH1 with structural genes from different genotypes[71] (E). The HCV genome is represented on top for comparison purposes**.** AKA (also known as) indicates the nomenclature commonly used in the HCV research community for the replicons represented.

Chimeric replicons can be intra or intergenotypic, where intergenotypic replicons usually present lower titers due to incompatibilities of proteins derived from different genotypes. The J6-JFH1 replicon (J6/C) (Figure 1.4 E) delivers the highest yield for HCVcc production since both genomes derived from GT2a (intragenomic chimeric replicon). The problem of genetic incompatibility in intergenotypic chimeras can be overcome by adapting the replicon to cell culture along passages, resulting titer-enhancing mutations

(TEMs) and an increased viral titers[19,20,52], although this is undesirable. Particles produced with chimeric replicons have physical properties similar to HCVwt and are capable of infecting new target cells *in vivo* and *in vitro*, allowing complete life cycle progression, including viral entry, replication, packaging, assembly, maturation and release of particles.

Another major hallmark in replicon systems was the development of tagged replicons. In this case, replicons are associated to reporter genes, which makes it possible to monitor cells capable of RNA replication. Furthermore, tagged replicons are useful to study and track genome replication mechanisms, viral particles production and cell infection in living cells[52,72]. In addition, tagged replicons have contributed to the identification of new functionalities of proteins involved in viral life cycle[73] and to track functional HCV replicating complexes[72]. To develop a tagged HCV replicon, Moradpour and colleagues[72] mapped permissive sites for insertion of an external green fluorescent protein (GFP) into the non-structural genomic sequence HCV. These efforts revealed that the NS5A C-terminal region is flexible and tolerant to accommodate insertions, and two permissive sites were identified in viable replicons for GFP insertion with minimal effect on the replication function[72,74]. The newly tagged replicon expressing NS5A-GFP fusion protein allowed direct visualization of HCV replication by fluorescence microscopy enabling studying HCV in living cells[72]. Furthermore, in 2014, a genetic footprint of the entire HCV genome in high-resolution was conducted profiling potential regions for tag insertion along the whole viral genome[73]. These results revealed additional regions prone to insertions in the core, E2, p7, NS2, and corroborated the two tolerant regions in the NS5A C terminus reported by Moradpour *et al.* [72].

HCV replicons tagged with reporter genes function as bioprobe since they allow the visualization of HCV permissive cells. When the reporter gene encodes a fluorescent protein, the bioprobe has a transducer component to convert the recognition of a HCV replicating cell into a signal, through the expression of fluorescent protein fused with a viral protein. Moreover, tagged replicons may allow higher sensitivity, selectivity and rapid responsiveness in the detection of HCV replicating cells[75,76] relative to selection markers.

1.5. Translation mechanisms of RNA

When RNA viruses infect cells and their genome arrives into the cytoplasm, their genes are translated by mechanisms of initiation and regulation of protein synthesis[77,78]. This is valid for *in vivo* generated RNA molecules as well as for *in vitro* synthesized RNA. For translation initiation, transcripts are recognized by eukaryotic translation initiation factors (eIFs) and ribosomal subunits, and the ribosome is directed to the start codon (AUG)[79,80]. Translation initiation can proceed by a cap-dependent or cap-independent mechanism.

1.5.1. Cap-dependent mechanism

In eukaryotic cells, translation initiation is generally mediated by a cap-dependent mechanism, that takes place not only for cellular transcripts but also for almost all viral mRNAs[81]. Capping is vital to mRNA because it is responsible for gene expression modulation by splicing, transportation, stabilization[82–84], protection against exonucleases, translation initiation promotion and regulation[81,85]. This mechanism uses a 5´terminal nuclear modification, a N7-methylated guanosine triphosphate ($m^7G(5´)ppp(5´)N$- cap)[82–85] that is a 7-methylguanosine residue connected by a 5´ to 5´triphosphate bridge to mRNA[79,86]. The cap is synthesized *in vivo* and added to the RNA by three sequential enzymatic reactions, involving the RNA triphosphatase (TPase), the RNA guanylyltransferase (GTase) and the guanine-N7 methyltransferase (guanine-N7 MTase)[84,86,87]. Capped-viruses can use this host capping mechanism or an alternative virus-specific capping mechanism[88]. Alternative to *in vivo* cap synthesis, there is a great variety of synthetic cap analogs, such as anti-reverse cap analogs (ARCAs), which are essential to add to *in vitro* synthesized RNAs lacking cap-independent translation[84,89].

When RNA translation occurs in a cap-dependent system (Figure 1.5 A), it starts through the formation of the translation eukaryotic initiation factor (eIF)-4F complex. This complex is composed by three proteins (EIF4E, EIF4A and EIF4G) that recognize the cap structure, binds to RNA, mediates the recruitment of 40S ribosomal subunit and the formation of 43S preinitiation complex[78,82,90,91]. The 43S complex scans the RNA in the 5´to 3´direction until the initiator Met-tRNA identifies the initiation codon (AUG), by codon-anticodon base pairing, and forms 48S initiation complex. Finally, when the 60S ribosomal subunit merges with the 48S complex, it forms the elongation complex (the 80S ribosome) starting the elongation stage of peptide synthesis. Translation termination occurs when the ribosome reaches a stop codon and the ribosome is recycled[78,82,90].

1.5.2. Cap-independent mechanism

Alternative to cap-dependent mechanisms, translation can be mediated by cap-independent mechanisms, which are commonly found in positive-strand uncapped RNA viruses or in mRNA when cells are exposed to stress[77,78]. In these cases, translation initiation signal is given by a cis-regulatory complex RNA element, the internal ribosome entry site (IRES), generally located at 5´untranslated region (UTR) of the RNA. For transcripts lacking a cap, the 40S ribosomal subunit can bind directly to the IRES (Figure 1.5 B) through RNA-RNA interactions, or by interacting with eIFs and RNA binding proteins (RBPs) (Figure 1.5 C) via RNA-protein interactions[78,82,90].

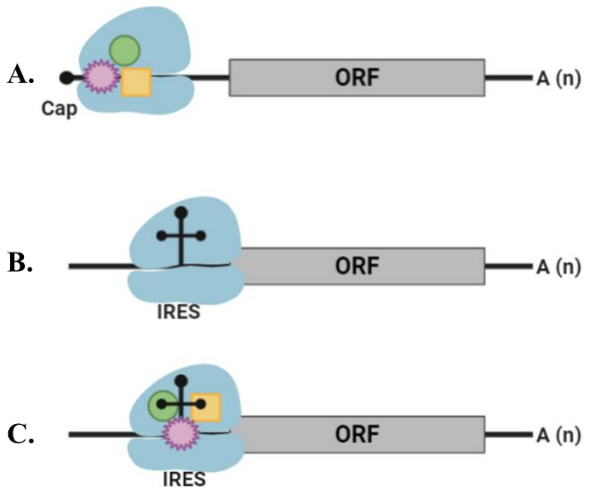

Figure 1.5 - Mechanisms of translation initiation in eukaryotic RNA. Cap-dependent mechanisms, where the cap structure requires eIF association and ribosome recruitment to initiate translation (A). Cap-independent mechanism, where IRES structures recruit directly the 40S ribosomal subunit (B). Cap-independent mechanism, when IRES structures recruits ITAFs allowing ribosome recruitment (C). Figure created with BioRender.com.

There are numerous IRES elements derived from different viruses presenting common features, such as functioning autonomously as a module entity and exhibiting their activity outside of its native sequence, even when located between two ORFs. Despite the modularity, it is essential that an IRES remains complete to conserve its multidomain organization and structural integrity[78]. The IRES of different viruses share little homology[78,82]. The differences are responsible for distinct RNA structures and primary sequences[78,92]. These structures dictate whether direct or protein mediated recruitment of 40S ribosome subunit takes place. These cellular RNA-binding proteins, so called IRES *trans*-acting factors (ITAFs)[93], includes eIFs and RBPs[94].

Viral IRES have been classified into four classes (I to IV, Table 1.1) and a fifth unassigned class, according to structural organization, length, nucleotide sequence and initiation mechanism[78,95,96]. Regardless of their classes, all IRES retain structural flexibility, which is essential to acquire distinct conformations when binding to specific ligands or when exposed to environmental signals[77,78].

Table 1.1- Typed of class-assigned IRES

	Viruses	Main characteristics
Type I	Enterovirus, such as the poliovirus (PV)	- 450 nt long and organized in five domains (II- VI); - Requires EIF2, EIF3, EIF4A and EIF4G[78].
Type II	Encephalomyocarditis virus (EMCV) and the foot-and-mouth disease virus (FMDV)	- 450 nt long, divided into modular domains (2-5), which are responsible to direct translation initiation machinery to the correct start codon[95], since it is possible to have multiple start codons; - Involves the same factors as IRES type I[78].
Type III	Hepatitis A virus (HAV)	- Contains more complex secondary and tertiary structures; - Requires few eIFs, such as EIF4E and EIF4G[78].
Type IV	HCV-like IRES, also present in teschovirus	- Compact and complex element with around 230-420 nt long[97]; - Presents two complex domains (II and III) and pseudoknots[95], allowing a direct interaction between the RNA and 40S ribosomal subunit[91]; - EIF2 and EIF3 dependent[78,98].

nt: nucleotides

Hepatitis C virus IRES is a hepatocivirus IRES, similar to type IV IRES of picornavirus. It is a flexible and dynamic structure of 340 nucleotides length present at 5´UTR of the RNA viral genome[78]. It contains four domains I to IV[95] with distinct functions in the recruitment of the translation machinery. Domain III is the largest and it is responsible for 40S ribosomal subunit recruitment, that docks on domain II. Domain IV contain the start codon at the loop. IRES from different HCV genotypes present differential translation efficiencies[78,91,95,99,100].

1.6. Context, aim and strategy

The work of this Master thesis was part of a larger research project aiming at developing robust and reliable cell culture systems of highly permissive hepatic cell lines to replicate and propagate HCV wild type. These cell lines were previously developed through immortalization of primary human hepatocytes (PHH). In that context, this thesis integrates the work task of developing and validating the molecular tools for screening hepatic cell lines highly competent for HCV replication and assembly, and implementing the protocols for producing and handling HCVcc.

To have an efficient method to deliver RNA molecules into cells, we started by optimizing the transfection conditions using Lipofectamine MessengerMAX transfection reagent (Part 1). Then, an *in vitro* transcription protocol was implemented and validated to produce the RNA transcripts, namely the HCV replicons and internal reporter controls (Part 2). Also, we developed a new HCV full-length replicon tagged with GFP, to function as a bioprobe to distinguish HCV permissive from non-permissive cells, through a fluorescent signal (Part 3). Implementation of an immunostaining protocol to validate the tagged replicon (Part 4).

2. MATERIALS AND METHODS

For the entire materials and methods section, kits, reagents, and equipment were used following the instructions recommended by the respective manufacturer, unless otherwise stated.

2.1. Plasmids

All plasmids constructed during this work, and their main transcriptional units are showed in Figure 7.1 and 7.2, in annexes. Primers, templates and double-stranded DNA (dsDNA) fragments (gBlocks and GenScript plasmids) used for plasmid construction are given in Table 7.1 and 7.2, also in annexes.

pCI-NEO (Promega Corporation, Madison, WI, USA) is a mammalian expression plasmid containing the cytomegalovirus (CMV) promoter followed by a T7 promoter upstream of a multiple cloning site (MCS). This plasmid was used as backbone for the construction of two other plasmids (pCI-NEO_GFP and pCI-NEO_mCherry) by cloning, into the EcoRI restriction site of the MCS, the reporter genes of the enhanced green fluorescent protein (eGFP- referred as GFP from now on) and mCherry sequences, respectively, amplified by PCR. Reporter sequences sources were the GFP from pRRLSIN.cPPT.PGK-GFP.WPRE (Addgene plasmid #12252, Watertown, MA, USA), and the mCherry from pPuro_mCherry (plasmid established by Ana Oliveira, ACTU, iBET). Additionally, a T7 terminator sequence was synthesized by integrated DNA technologies (IDT, Dresden, Germany) and included at the end of the reporter sequence at the MfeI restriction site, originating pCI-NEO_GFP_T7.Term and pCI-NEO_mCherry_T7.Term. These two plasmids were used as internal positive controls.

pCI.NEO_GFP_T7.Term_dBsrGI was established by site directed mutagenesis of pCI.NEO_GFP_T7.Term, to introduce a point mutation to abolish the BsrGI restriction site existing at the end of the GFP sequence. This plasmid was used as a control to compare GFP functionality of non-mutated GFP (pCI-NEO_GFP_T7.Term) with the mutated gene (GFP_dBsrGI), since GFP_dBsrGI was present in the tagged replicon (pJ6/C_GFP).

A set of IRES sequences were added to pCI-NEO_GFP_T7.Term upstream of the GFP sequence, generating five different plasmids where the reporter translation is driven by an IRES: i) pCI-NEO_GFP_T7.Term_IRES-PV has the poliovirus IRES sequence from pcDNA3 RLUC POLIRES FLUC (Addgene, plasmid #45642); ii) pCI-NEO_GFP_T7.Term_IRES-EMCV carries the encephalomyocarditis virus IRES derived from pMIG (Addgene, plasmid #9044); iii) pCI-NEO_GFP_T7.Term_IRES-HAV carries the hepatitis A virus IRES, synthesized by GenScript (Piscataway, NJ, EUA); iv) pCI-NEO_GFP_T7.Term_IRES-HCV harbors the IRES from the hepatitis C virus obtained from pJ6/C; v) pCI-NEO_GFP_T7.Term_IRES-HIV-I.Gspacer contains the 5´UTR of HIV-1 from pRRLSIN.cPPT.PGK-GFP.WPRE (Addgene, plasmid #12252) fused to a glycine spacer (G spacer) downstream of the IRES. The

IRES sequences of PV, EMCV, HCV and HIV-1 were amplified by PCR and cloned into the NheI restriction site. These plasmids were used as an internal positive control and allowed a side-by-side comparison the activity of the different IRES.

Plasmid pJ6/C contains the full-length chimeric HCV replicon J6/C described in [70]. This plasmid was kindly provided by Dr. Thomas Pietschmann (TWINCORE, Hannover, Germany). pJ6/C_GFP is the full-length J6/C chimeric replicon tagged with a GFP reporter gene flanked by G spacers at the proline 2390 position in NS5A, as previously described in [72]. The GFP reporter sequence flanked by G spacers and the pJ6/C sequences between the restriction site of RsrII and BsrGI was synthesized by GenScript (Piscataway, NJ, EUA), and cloned into pJ6/C at the same restriction sites. This plasmid were used for HCV replication and HCVcc production.

2.2. Cloning procedures

For all plasmids derived from pCI-NEO, ligation reactions were carried out using In-Fusion HD Cloning system (Takara, Mountain View, CA, USA). For pCI.NEO_GFP_T7.Term_dBsrGI, pCI-NEO-GFP_T7.Term_IRES-HAV and pJ6/C_GFPinNS5A plasmids, ligation reactions were conducted using T4 DNA Ligase (NEB, Ipswich, MA, EUA).

DNA fragment amplification was performed by PCR using Phusion High-Fidelity DNA Polymerase (Finnzymes Oy, Vantaa, Finland) in a Biometria T3 Personal Thermocycler (Biometria, Göttengen, Germany). Cloning vectors were digested using NEB enzymes and buffers. Primers and double-stranded DNA fragments (gBlocks) were custom-made synthesized by IDT (Dresden, Germany).

Isolation of the fragments produced by PCR or restriction reactions was carried out using 0.7% (w/v) agarose gels (NZYTech, Lisbon, Portugal), prepared in TAE buffer (Qiagen, Hilden, Germany) and stained with 0.5 µL/mL RedSafe Nucleic Acid Stainng Solution (INtRON Biotechnology, South Korea). Gels were visualized with a GelDoc XR+ system (BioRad, Hercules, CA, USA). Fragments were purified using NucleoSpin Gel and PCR clean-up kit (Macherey-Nagel, Düren, Germany).

2.3. Site directed mutagenesis

To generate pCI.NEO_GFP_T7.Term_dBsrGI, a site directed mutagenesis protocol [101] was employed using Phusion High-Fidelity DNA Polymerase (Finnzymes Oy), 5'-phosphorylated primers for inverted PCR, DpnI (NEB) restriction enzyme to digest the template DNA and T4 DNA Ligase (NEB) for circularization of the PCR product.

2.4. Bacteria strains and culture media

NEB 5-alpha Competent *E. coli* (NEB) bacteria were used for cloning reactions and plasmids amplification. Liquid and agar culture media were prepared with Fast-Media Amp LB or FastMedia Amp Agar (InvivoGen, San Diego, CA, EUA), containing the antibiotic appropriate for bacteria selection.

2.5. Plasmid purification and quality control

Plasmids were purified in a small scale ("mini-preps") with GeneJET Plasmid Miniprep Kit (Thermo Scientific, Waltham, MA, USA), and in a second step at larger scale ("maxi-preps") using Genopure Plasmid maxi kit (Roche Applied Science, Penzberg, Germany). Each new plasmid was preserved in bacteria banks at -80 ºC in 15% glycerol (Sigma-Aldrich, St. Louis, MO, USA).

DNA concentration was quantified using Nanodrop 2000C spectrophotometer (Thermo Scientific). DNA purity and integrity were analyzed by measuring the Abs_{260nm}/Abs_{280nm} and Abs_{260nm}/Abs_{230nm} ratios, and by electrophoresis gel run, respectively. DNA working banks were produced and stored at -20 ºC. All generated plasmids were sequenced by Sanger sequencing using Eurofins Genomics services (Ebersberg, Germany).

2.6. Cell Lines and culture conditions

Huh-7.5 cell line[102] is a clone derived from Huh-7[103] human hepatoma cell population (JCRB0403, Japanese Collection of Research Bioresources). This cell line was used as representative of a permissive hepatic cell line for all the studies and optimizations carried out in this thesis.

293T cell line (ATCC, American Type Cell Collection, CRL-3216) is derived from the Human Embryonic Kidney 293 (HEK 293) cell line[104], and constitutively expresses the SV40 large T antigen[105]. This cell line was used to evaluate GFP functionality of pCI.NEO_GFP_T7.Term_dBsrGI.

All cells were cultured in adherent conditions in standard polystyrene treated cell culture flasks (T-flasks, Sarstedt, Nümbrecht, Germany) with Dulbecco's modified Eagle's medium (DMEM, Corning, Corning, NY, USA) supplemented with 10% (v/v) fetal bovine serum (FBS, Gibco, Carlsbad, CA, USA). Cells were maintained in a humidified atmosphere at 37 °C with 8% (v/v) CO_2.

Working cell banks were established in FBS containing 10% (v/v) of dimethyl sulfoxide (DMSO, Sigma-Aldrich, St. Louis, MO, USA) and maintained at -80 ºC.

2.7. Cell concentration and viability

Cell concentration and viability were determined by the trypan blue exclusion method. Cells were diluted in 0.1% (v/v) trypan blue (Sigma-Aldrich) solution in phosphate-buffered saline (PBS) (Gibco), and

manually counted using a Fuchs-Rosenthal hemacytometer (Marienfield-Superior, Lauda-Konigshofen, Germany) on an inverted microscope (Olympus, Japan).

2.8. *In vitro* transcription

To generate RNA molecules of the HCV replicons, reporter controls or IRES-based translation system, a protocol of *in vitro* transcription was implemented. First, 20 µg of plasmid DNA were digested using an appropriate restriction enzyme (NEB). The resulting linearized DNA was column purified in QiAprep Spin Miniprep kit (Qiagen) and eluted in 60 µl of RNAse/DNAse free water (Fisher Scientific International, Inc., Pittsburgh, PA, USA). In a second step, the *in vitro* transcription was performed using 2 µg of linearized DNA, 20 µL of 5x rabbit reticulocyte lysate equivalent buffer (5xRRL), 12.5 µL rNTP-mix (at proportion of 1 rATP: 1 rUTP: 1 rCTP: 1 rGTP, Promega Corporation, Madison, Wisconsin, USA), 2.5 µL RNASIN (Promega) and 5 µL of RNA T7 polymerase (Promega); volumes are presented per reaction basis. The 5xRRL buffer was prepared as it follows: i) 400 mM HEPES (pH 7.3-7.5, Fisher Scientific International, Inc.), ii) 60 mM MgCl2 (Thermofisher), iii) 10 mM Spermidine (Sigma) and iv) 200 mM DTT (Sigma) in RNAse/DNAse free water. When necessary, an Anti-Reverse Cap Analog (ARCA) 3′-O-Me-m7G(5′) ppp(5′)G (NEB) was also added to this reaction. The reaction was incubated at 37º C, for 2 hours in a ThermoMixer (Eppendorf, Germany). After the incubation period, an additional 2 µL of RNA T7 polymerase were added for a transcription boost. In the final step, DNA was degraded by the addition of 7.5 µL DNase (Promega) and incubated for 30 minutes at 37º C. The resulting RNA was column purified using the NucleoSpin RNA Clean-up kit (Macherey & Nagel) and eluted in 50 µl of RNAse/DNAse free water. RNA concentration was determined using Nanodrop 2000C spectrophotometer and the integrity was evaluated by visualization in agarose gel at 0.7 %. RNA was aliquoted and stored at -80 ºC until further use.

2.9. Adherent cell transfection procedure

2.9.1. Transfection with lipofectamine transfection reagent

Lipofectamine MessengerMAX transfection reagent (Invitrogen) was used to deliver RNA molecules into Huh-7.5 cell lines. Cell seeding was performed at concentration of $6.8x10^4$ cells/cm^2, in 24-well plates. Cell transfection was performed at 24 hours post-seeding. Lipofectamine (LF), total RNA and lipofectamine to total RNA ratios varied across assays. As reporters and/or internal controls CleanCap EGFP mRNA or CleanCap mCherry mRNA (5-methoxyuridine) both from TriLink BioTechnologies (San Diego, CA, USA), or pCI-NEO derived transcripts were used. As HCV replicons J6/C^{71} and its tagged derivative J6/C_GFP were transfected. Transfection efficiency was determined at 24, 48 or 72 hours post-transfection by flow cytometry analysis BD FACSCelesta Flow Cytometer (BD, Franklin Lakes, NJ, USA).

2.9.2. Transfection with polyethylenimine transfection reagent

To compare non-mutated and mutated GFP, both plasmids were transfected into adherent 293T cells using pCI-NEO_GFP_T7.Term and pCI-NEO_GFP_dBsrGI. Cell seeding was performed at a concentration of $6x10^4$ cells/cm^2. After 24 hours, cells were transfected using polyethylenimine (PEI, Linear 25kDa, Polysciences, Inc., Warrington, PA, USA) as transfection reagent, using a 1:1.5 (w/w) ratio of DNA:PEI, and 5 µg of total DNA per million of cells. DNA and PEI mix was prepared in serum-free DMEM. DNA mix was filtered through a 0.22 µm pore-size cellulose acetate filter and added to PEI mix. After 12 minutes of incubation at room temperature, the final transfection mix was added to culture medium of adherent cells. Transfection efficiency was determined at 48 hours post-transfection by flow cytometry analysis BD FACSCelesta Flow Cytometer.

2.10. Cellular RNA extraction and cDNA synthesis

Total cellular RNA extraction was performed using QIAamp RNeasy Mini kit (Qiagen) and eluted in 60 µl of RNase-free water. RNA was quantified using Nanodrop 2000C Spectrophotometer (Thermo Scientific) and stored at -80 ºC.

For cDNA synthesis, Transcriptor High Fidelity cDNA Synthesis kit (Roche Applied Science) was used to reverse transcribe 2 µg of total RNA using anchored-oligo(dT)18 primers. Synthesized cDNA was aliquoted and stored at -20 ºC, until further use.

2.11. Real-Time quantitative PCR (RT-qPCR)

RNA transcripts were quantified by real-time quantitative PCR (RT-qPCR) using the $2^{-\Delta Ct}$ method[106] and the Ribosomal Protein L22 (RPL22) as reference gene. RT-qPCR reactions were performed using the LightCycler 480 Real Time PCR System (Roche Applied Science) and LightCycler 480 SYBR Green I Master mix (Roche Applied Science). Primers are listed in Table 7.3, in annexes.

2.12. Cell fixation, permeabilization and staining

To evaluate HCV replication and viral protein production, the NS3 protein was quantified by immunofluorescence in fixated and permeabilized cells. A total of $2x10^4$ cells were harvested and pelleted at 300 *g* for 8 minutes in a microcentrifuge tube. Then the pellet was washed with 1.5 mL of wash buffer (PBS with 2% FBS (v/v)). Centrifugation was repeated and the supernatant discarded. Then 0.5 mL of Fixation Buffer (BioLegend, San Diego, CA, USA) were added per tube and incubated for 20 minutes at room temperature in the dark. Cell permeabilization was performed by resuspending fixated cells in 1.5 mL of 1x diluted Intracellular Staining Permeabilization Wash Buffer (10x) (BioLegend) in RNAse/DNAse free water, and centrifuged at 300 *g* for 8 minutes. This process was repeated twice. Fixated and permeabilized cells were resuspended in wash buffer and stored at 4 ºC until use.

Fixated cells were stained against the HCV NS3 using the Anti-Hepatitis C Virus NS3 antibody [8 G-2] (Abcam, Cambridge, England), diluted in wash buffer and incubated for 1 hour at 4 ºC. Then, cells were washed using wash buffer and incubated with the secondary antibody, Alexa Fluor 488 Goat anti-mouse IgG (Invitrogen), diluted 1:20 in wash buffer, for 30 minutes at 4 ºC. Finally, cells were washed and analyzed by flow cytometry (BD FACSCelesta Flow Cytometer).

3. RESULTS

The work of this thesis aimed at developing and validating a set of molecular tools for high-throughput screening of hepatic cell lines highly competent for HCV replication and assembly. In particular, we sought for establishing a full-length replicon based on J6/C tagged with a GFP reporter to distinguish cells replicating HCV from those not replicating the virus. Alongside, we also aimed at implementing and optimizing the protocols to produce and handle HCVcc. Within this scope, four work lines were followed. We started by i) optimizing the transfection method for intracellular delivery of RNA using lipofectamine MessengerMAX and ii) implementing an *in vitro* transcription protocol for *in vitro* synthesis of RNA, and constructing of the necessary positive controls. Then we proceeded with iii) the construction and evaluation of the tagged replicon with a GFP reporter, and iv) implemented a fixation, permeabilization and staining protocol to evaluate and validate the tagged replicon.

3.1. Optimization of RNA transfection using lipofectamine

Lipofectamine MessengerMAX transfection reagent was chosen to deliver the RNA molecules in to Huh-7.5 cell line, since it was described as a highly efficiency delivery vehicle for RNA in difficult to transfect cells. To identify the best transfection conditions, two different ratios of lipofectamine to RNA (LF:RNA) were tested: 1 µL of LF to 333 ng of RNA and 1 µL LF to 666 ng of RNA, as recommended by the supplier. At the first stage, a commercial RNA stock was used (CleanCap EGFP mRNA) at three different concentrations: 250, 500 and 1000 ng per well, in 24-well plates. The transfection efficiency was evaluated at 24 and 48 hours post-transfection.

The results showed that lipofectamine was efficient at delivering RNA molecules to Huh-7.5 cells, achieving transfection efficiencies higher than 70% under all tested conditions (Figure 3.1). The best transfection conditions occurred when using the ratio of 1 µL of LF to 333 ng of RNA, for both 500 and 1000 ng of RNA with transfection efficiencies around 90% of GFP positive cells. For both of LF:RNA ratios tested, the condition using 1000 ng of RNA resulted in a slightly higher transfection efficiency, although with an evident cell death increase, when comparing to the non-transfected control and the condition with 500 ng of RNA. Therefore, the ratio of 1:333, using 500 ng of RNA was selected as the best transfection condition. Additionally, the results did not show major differences in percentage of GFP positive cells between 24 and 48 hours post-transfection.

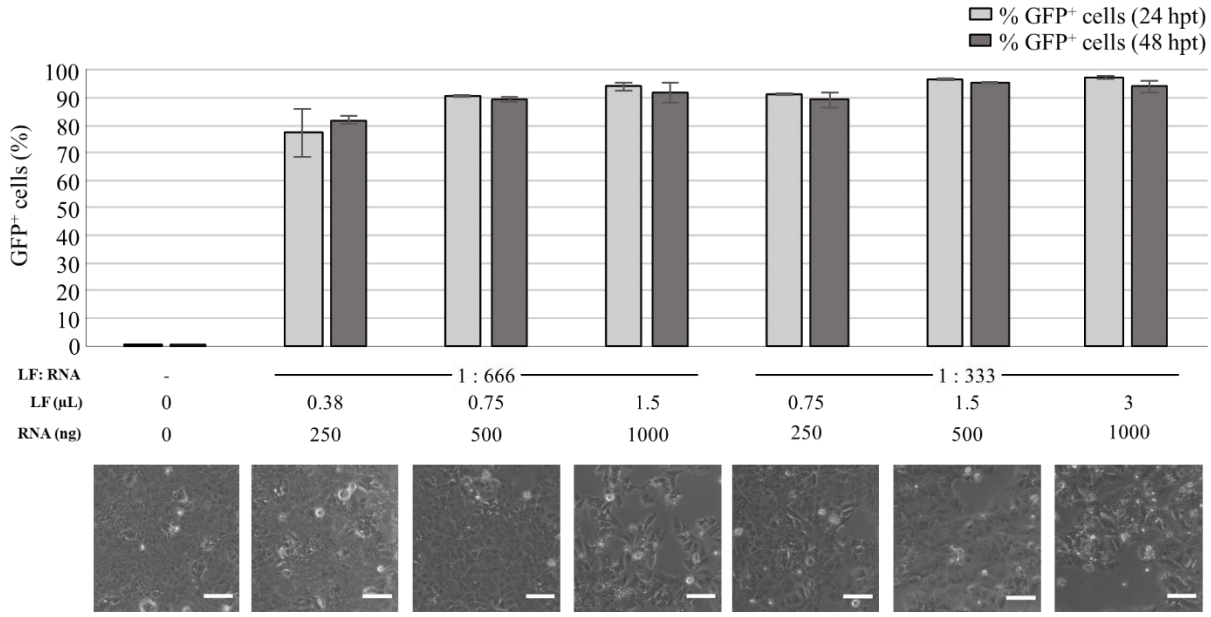

Figure 3.1 – Optimization of RNA transfection into Huh 7.5 cells using Lipofectamine MessengerMAX. Two lipofectamine to RNA (LF:RNA) ratios were tested of 1 µL LF to 333 and 666 ng of RNA, using 250, 500 and 1000 ng of RNA, per well of 24-well plates. The percentage of GFP positive cells was determined by flow cytometry and is shown as average ± standard deviation of two technical replicates. Panels below the chart show phase-contrast microscopy images of the corresponding Huh-7.5 cells at 48 hours post-transfection. Scale bar = 100 µm.

3.2. *In vitro* transcription protocol

After defining a delivery vehicle for RNA transfection, an *in vitro* transcription (IVT) protocol was implemented to synthesize the RNA molecules of the tagged replicon. The general framework for this protocol is shown in Figure 3.2.

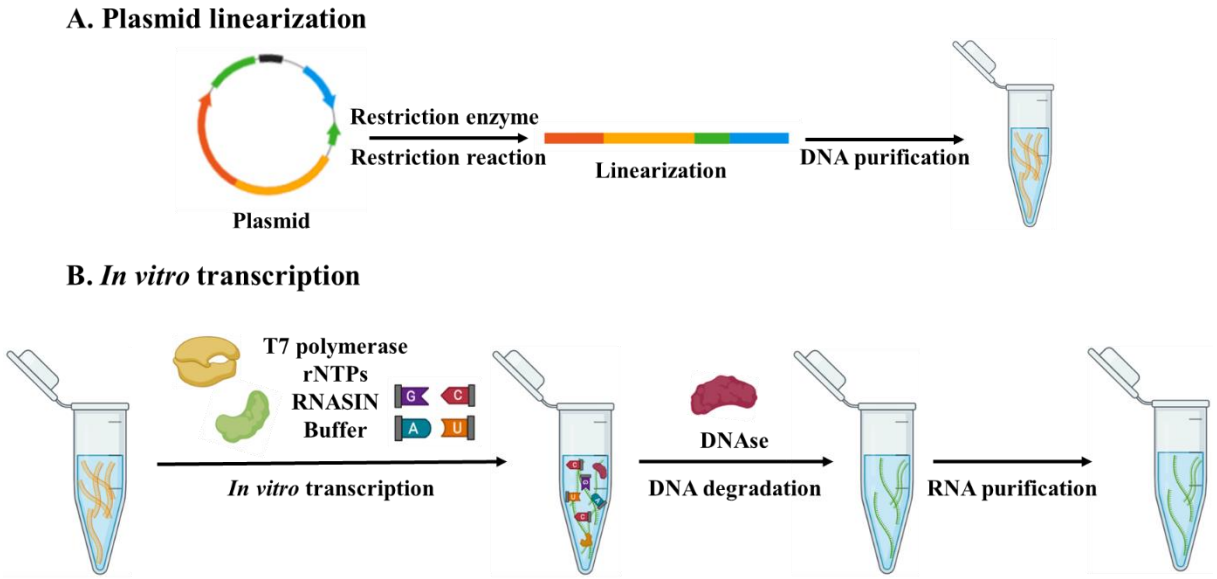

Figure 3.2 - *In vitro* transcription protocol implemented in this work. The protocol has two major steps: plasmid linearization through a restriction reaction, followed by DNA purification in column (A) and the *in vitro* transcription reaction (B), which uses T7 polymerase for RNA synthesis and contains all the remaining components needed for the RNA synthesis (ribonucleotide triphosphates (rNTPs), RNASIN and buffer). The DNA template is then degraded, and the RNA is finally purified in column purification. Figure created with BioRender.com.

At the end of the IVT protocol, the RNA yields and purity were quantified (Table 3.1). The results showed that lower length transcripts, with around 1 kb long, deliver higher yields, than longer transcripts, with around 10 kb. Overall, the produced RNA presented a good purity, since the absorbance ratios Abs_{260nm}/ Abs_{280nm} were around 2.1-2.2 which indicates that RNA was protein free, and the ratio Abs_{260nm}/ Abs_{230nm} was between 2.1 and 2.3 indicating that RNA was free from other contaminants, namely chaotropic salts and phenol.

The RNA integrity was evaluated by visualization in an agarose gel (Figure 3.3) based on the smearing pattern. Longer transcripts seemed to present higher smearing than smaller transcripts. Although, in both cases, the smear was small, indicating an overall good integrity.

Table 3.1 - *In vitro* transcription yields and spectroscopic ratios.

Transcripts length	RNA concentration (ng/ µL)	Abs_{260}/ Abs_{280}	Abs_{260}/ Abs_{230}
Negative control[a)]	26.9	2.03	1.51
1 kb [b)]	2523.6	2.17	2.20
	2041.3	2.17	2.21
	2465.9	2.17	2.17
	1932.2	2.16	2.23
10 kb [c)]	729.0	2.15	2.19
	1261.4	2.14	2.16
	1180.4	2.14	2.18
	1291.8	2.14	2.14

[a)] IVT negative control reaction contains all the compounds necessary for the IVT reaction, except T7 RNA polymerase.
[b)] 1 kb transcript correspond to the internal GFP control, further explained in section 3.2.1.
[c)] 10 kb transcripts correspond to the J6/C replicon and its tagged derivative, further explained in section 3.3.

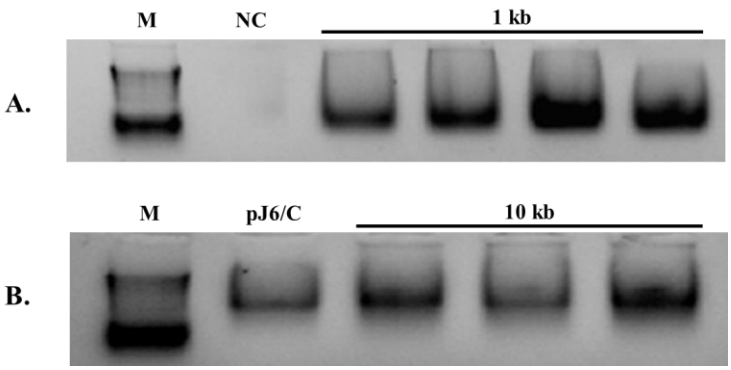

Figure 3.3 – Electrophoresis of RNA molecules synthesized IVT. Agarose gel profile of smaller transcripts (around 1 kb) (A), and longer transcripts, with around 10 kb (B). M- DNA molecular weight ladder. NC: negative control corresponding to the reaction containing all the compounds necessary for the IVT reaction, except T7 RNA polymerase

3.2.1. Internal positive control

In this work we constructed two reporter control plasmids, the pCI-NEO_GFP_T7.Term and the pCI-NEO_mCherry_T7.Term (Figure 3.4). These plasmids served several purposes, pCI-NEO_GFP_T7.Term (Figure 3.4 A) was used for the implementation of the *in vitro* transcription protocol (see Table 3.1 and Figure 3.3) since the visualization of the reporter protein encoded by the *in vitro* synthesized transcripts provided an easy readout to evaluate the functionality of the IVT protocol. In addition, we needed a co-transfection control to use with the tagged replicon to enable a normalization of the replicon signal to the transfection efficiency. Therefore, pCI-NEO_GFP_T7.Term could not be used for

that purpose, since it also expresses the GFP protein. Instead, the pCI-NEO_mCherry_T7.Term (Figure 3.4 B) construction was established to be used as a co-transfection internal control independent from replicon tagged whit GFP. Although, commercial RNAs, such as CleanCap EGFP and mCherry mRNA, suited the purpose of functioning as an internal control, we sought for a more cost-efficient alternative.

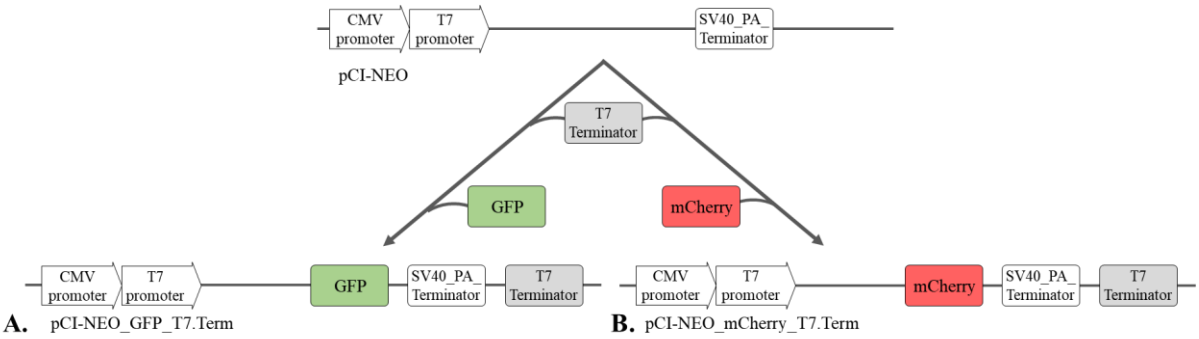

Figure 3.4- Construction of GFP and mCherry reporter control plasmids. Starting with pCI-NEO already containing the T7 promoter and poly-A terminator, and the T7 Terminator was added, followed by the addition of the GFP, to establish the pCI-NEO_GFP_T7.Term (A) or mCherry to established pCI-NEO_mCherry_T7.Term (B).

3.2.2. GFP translation mediated by cap-dependent mechanism: ARCA optimization

For the transcripts generated with pCI-NEO_GFP_T7.Term or pCI-NEO_mCherry_T7.Term (see Figure 3.4) to be translated, a cap-dependent mechanism is necessary. To test the translation initiation mechanisms, only pCI-NEO_GFP_T7.Term was used. Herein, we used a cap analog (ARCA) added to the IVT reaction mix at the concentration of 2, 5 and 8 mM, per reaction (Figure 3.5). The generated transcripts were transfected into Huh-7.5 cells using the ratio of 1 µL of LF to 333 ng of RNA, and 500 ng of RNA, previously defined as the optimum transfection condition (see Figure 3.1).

The addition of ARCA to the IVT reaction was found to be required for RNA translation, since there was no expression of the reporter in its absence. The best GFP translation condition occurred when using 8 mM of ARCA with an average of 66 % of GFP positive cells. Although the increase in ARCA concentration resulted into an increase in GFP positive cells, it never reached the results obtained with the commercial RNA of almost 90% of GFP positive cells.

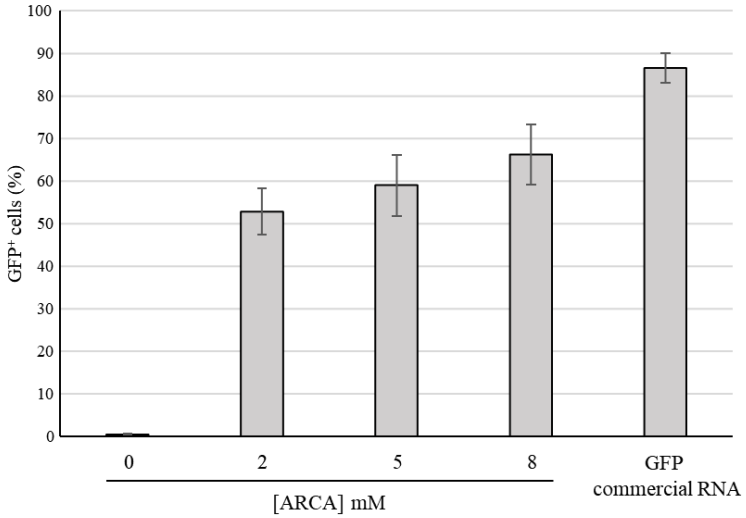

Figure 3.5 - Optimization of ARCA concentration in IVT for cap-dependent transcripts translation. Transfection was carried out using the best conditions defined previously of 500 ng of RNA per well of 24-well plates, at the ratio of 1 µL of LF to 333 ng of RNA. The percentage of GFP positive cell was determined by flow cytometer, at 24 hours post-transfection, and is shown as average ± standard deviation of three independent transcripts (IVT), all of which transfected three independent times (final N=9).

We took advantage of the several independently synthesized transcripts to further evaluate the assay variability, namely to distinguish the variability derived from *in vitro* transcription from that derived from transfection (Table 3.2 and 3.3). The results showed that the coefficient of variation, defined as standard deviation/average, was higher between the same transcript transfected at different times (intra-transfection variation), than when different transcripts were transfected at the same time (inter-transfection variation). These results demonstrated that the *in vitro* transcription protocol was reproducible given that most variability derived from the transfection and rather than from the IVT.

Table 3.2- Assessment of intra-transfection variation.

[ARCA] (mM)	Intra-transfection variation*							
	IVT 1		IVT 2		IVT 3			
	Av	CV (%)	Av	CV (%)	Av	CV (%)	Av	CV (%)
2	50.8	21.6	48.6	21.1	59.0	60.0	52.8	16.2
5	51.2	30.8	65.5	28.4	60.4	16.1	59.0	25.1
8	58.1	19.5	70.5	12.4	70.1	5.7	66.2	12.5
Commercial GFP RNA	83.8	4.7	90.6	6.2	85.2	6.1	86.5	5.7

***** Intra-transfection variation corresponds to three *in vitro* synthesized RNAs transfected independently (IVT 1, 2 and 3).
Av: Average.
CV: Coefficient of variation defined as standard deviation/average and shown in percentage.
IVT: *In vitro* transcription.

Table 3.3 - Assessment of inter-transfection variation.

[ARCA] mM	Intra- transfection variation*		Inter- transfection variation**	
	Av	CV (%)	Av	CV (%)
2	52.8	16.2	56.8	11.6
5	59.0	25.1	68.1	8.0
8	66.2	12.5	72.5	2.6
Commercial GFP RNA	86.5	5.7	84.8	3.0

***** Intra-transfection variation corresponds to three *in vitro* synthesized RNAs transfected independently (IVT 1, 2 and 3).
****** Inter-transfection variation corresponds to the three in vitro transcribed RNA transfected at the same time.
Av: Average.
CV: Coefficient of variation defined as standard deviation/average and shown in percentage.

To understand the lower percentage of GFP positive cells when transfecting with the *in vitro* transcribed RNA (see Figure 3.5), the intracellular levels of GFP mRNA were quantified by RT-qPCR (Figure 3.6). The results showed that transfecting with *in* vitro synthesized RNAs resulted in intracellular mRNA levels 3-fold lower than those obtained with the commercial GFP RNA.

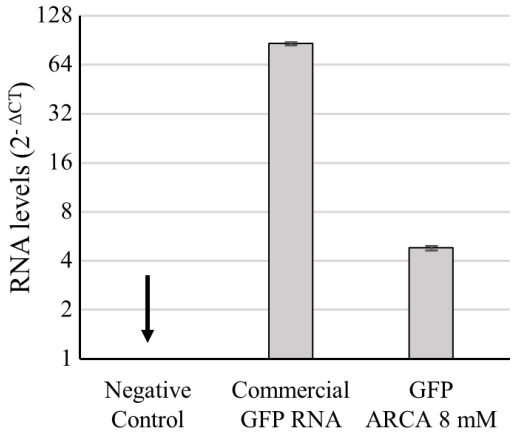

Figure 3.6 - Comparison of intracellular RNA levels when using commercial GFP RNA and *in vitro* synthesized GFP RNA. In commercial and in-house IVT synthesized GFP RNA, intracellular RNA levels were quantified using the $2^{-\Delta Ct}$ method and RPL22 as internal reference gene. Results are shown as average ± standard deviation of two technical replicates. The black arrow indicates the absence of RNA levels in the negative control, which corresponds to non-transfected cells.

To evaluate the cost-effectiveness of using an IVT transcript versus a commercial RNA as internal positive control, we calculated the cost of IVT with and without using 8 mM of ARCA per reaction (Table 3.4). We found that a IVT transcript costed 0.2 €/ µg of RNA, but when it is required ARCA the cost raises to 1.5 €/ µg of RNA, comparing to the commercial transcript which costed 3.6 €/ µg of RNA. Although the costs of IVT with ARCA was lower than using commercial RNA, it implies the IVT synthesis and results in lower transfection efficiencies. This can be particularly problematic when using this control in its final

setting which is co-transfecting the transcript simultaneously with tagged replicon. Therefore, the use of IVT transcript as an alternative to commercial RNA as internal co-transfection control was discarded.

Table 3.4 - Price of IVT reaction

		Cost per reaction (€)	
		W/O ARCA	**W/ ARCA**
Linearization step	Restriction enzyme	3.0	3.0
	DNA column	2.0	2.0
IVT step	ARCA	0.0	121.0
	T7 polymerase	7.0	7.0
	rNTP	2.1	2.1
	DNAse	0.6	0.6
	RNA column	7.2	7.2
	Buffers, and others*	1.0	1.0
	Cost (€) per µg of RNA**	0.2	1.4

***** 5xRRL, ethanol and RNAse/DNAse free water.
**The calculation was based on the reagent cost per IVT reaction, per an average of total µg of RNA synthesized per IVT reaction.
W/O: IVT reaction without ARCA.
W/: IVT reaction with ARCA

3.2.3. GFP translation mediated by cap-independent mechanism: IRES

To overcome the problem of low cost-effectiveness of the ARCA usage in IVT synthesized transcripts, the cap-independent mechanism was explored. Therefore, we sought for establishing our internal positive controls using IRES-dependent translation, which involves a cost of 0.2 €/ µg of RNA (see Figure 3.4). To guide the choice of the best IRES for the control transcript, the activity of five IRES was evaluated in pCI-NEO_GFP_T7.Term backbone. These were IRES of type I (PV), type II (EMCV), type III (HAV), type IV (HCV) and an unassigned class (IRES-like region present on HIV-1). Five new constructions were started, represented in Figure 3.7. However, the supply chain of many reagents and consumables was severely delayed due to the COVID-19 pandemic in the last months of this work, namely the DNA fragment commercially acquired to GenScript. Therefore, only four of these constructions was concluded at the time this thesis was delivered.

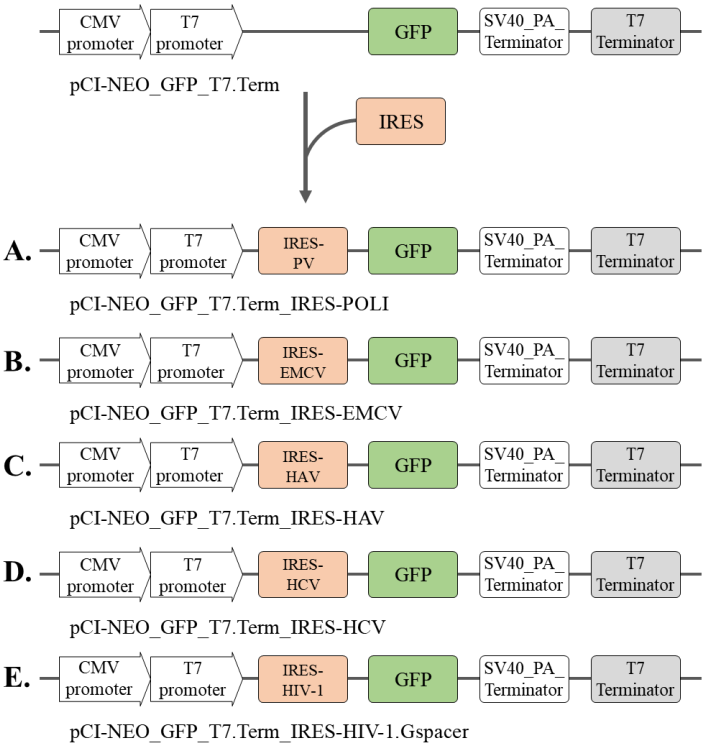

Figure 3.7 – Construction of GFP control plasmids for IRES-dependent translation. The IRES of poliovirus (PV, A), encephalomyocarditis virus (EMCV, B), hepatitis A virus (HAV, C), hepatitis C virus (HCV, D) and 5´UTR from retrovirus HIV-1 followed by G spacer fused with GFP (HIV-1, E), where added to pCI-NEO_GFP_T7.Term to enable cap-independent translation of the *in vitro* synthesized transcripts.

The efficiency of GFP translation under the regulation of the different IRES was evaluated by quantifying GFP positive cells, at 24 and 48 hours post-translation (Figure 3.8). GFP expression was absent in transcripts with HCV and HIV-1 IRES. PV and EMCV IRES supported the GFP translation initiation. However, both PV and EMCV IRES presented a reduced expression at 48 hours post-translation.

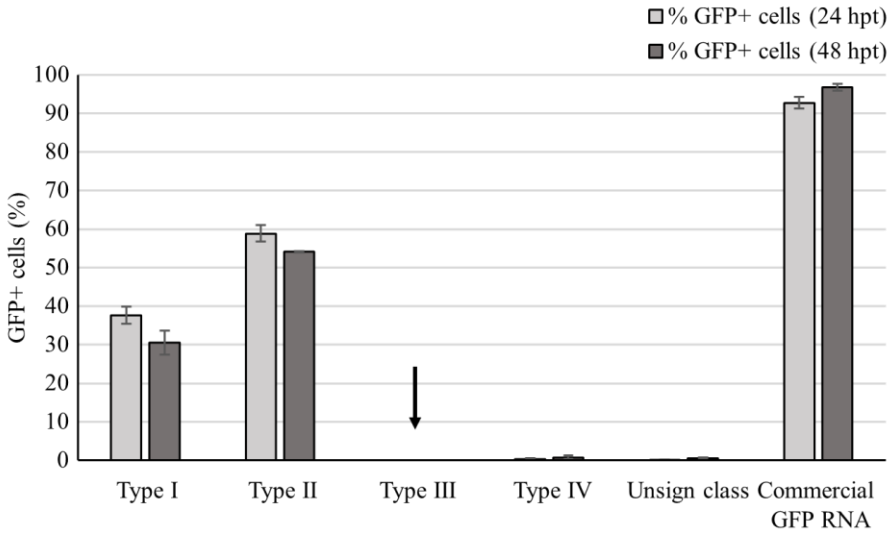

Figure 3.8 - Translation efficiency under the regulation of different IRES. The graph shows the translation efficiency of five IRES, type I (PV), type II (EMCV), type III (HAV), type IV (HCV) and the unassigned category (IRES-like region of HIV-1). Transfection was carried out using the best conditions defined previously of 500 ng of RNA per well of 24-well plates, at the ratio of 1 µL of LF to 333 ng of RNA. The percentage of GFP positive cell was determined by flow cytometer and is shown as average ± standard deviation of two replicates, at 24 and 48 hours post-translation. Black arrow corresponds to HAV IRES, for which plasmid construction was not finished.

3.3. Construction and evaluation of a full-length HCV replicon with a GFP tag

After completing the first set of objectives refereeing to transfection optimization, IVT implementation and internal controls development, we moved to the second stage of this work. We created a HCV full-length replicon tagged with a GFP reporter to function as a bioprobe in the screening of HCV competent cell clones. To this end, we started from the chimeric replicon J6/C and established J6/C_GFP, featuring GFP fused to NS5A (Figure 3.9). This GFP-NS5A fusion was previously reported in [72]. The J6/C chimeric replicon was chosen because it is the most efficient replicon in *in vitro* culture, for HCV replication and HCVcc particles production. The GFP sequence had to be inserted precisely at the proline 2390 position in NS5A and no other amino acid could be left from the cloning strategy. Therefore, we opted to have a synthesized DNA fragment with the exact configuration required and have it cloned using the closest restriction sites possible (RsrII and BsrGI). However, the GFP sequence had a BsrGI restriction site which prevented the cloning procedure. Therefore, a point mutation in GFP was introduced to delete this restriction site. This mutation consisted of the exchange TAC to TAT, both encoding a tyrosine. This codon was chosen as the second most used in human, the first being TAC, to minimize the impact in translation duo to codon usage bias.

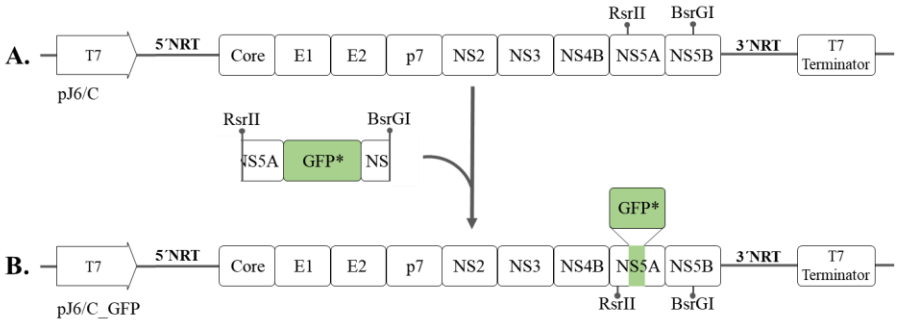

Figure 3.9 – Construction of J6/C replicon tagged with GFP. Starting with the plasmid of pJ6/C (A), the reporter gene GFP flanked by G spacers was added after the proline at the position of 2390 of NS5A gene, resulting in pJ6/C_GFP (B). The sequence of G spacers and GFP* was placed in frame with NS5A sequence, as described in[72]. To that end, the final sequence was design and obtained by commercial synthesis services using the closest restriction sites possible. The GFP* represents the mutated GFP, where BsrGI restriction site was eliminated.

Since the mutated GFP from the tagged replicon is affected by lower codon usage bias relatively to the non-mutated version, we compared the expression of mutated and non-mutated GFP to evaluate potential expression reduction from lower codon usage. Therefore, pCI-NEO_GFP_dBsrGI, containing the mutated GFP, was generated (Figure 3.10 A).

The plasmids containing the non-mutated and mutated GFP, pCI-NEO_GFP_T7.Term and pCI-NEO_GFP_dBsrGI respectively, were transfected in parallel into 293T cells (Figure 3.10 B). The result showed that the mutated version results in similar protein expression profile, thereby it can be used for pJ6/C_GFP cloning without expecting any impact on the reporter ability of GFP.

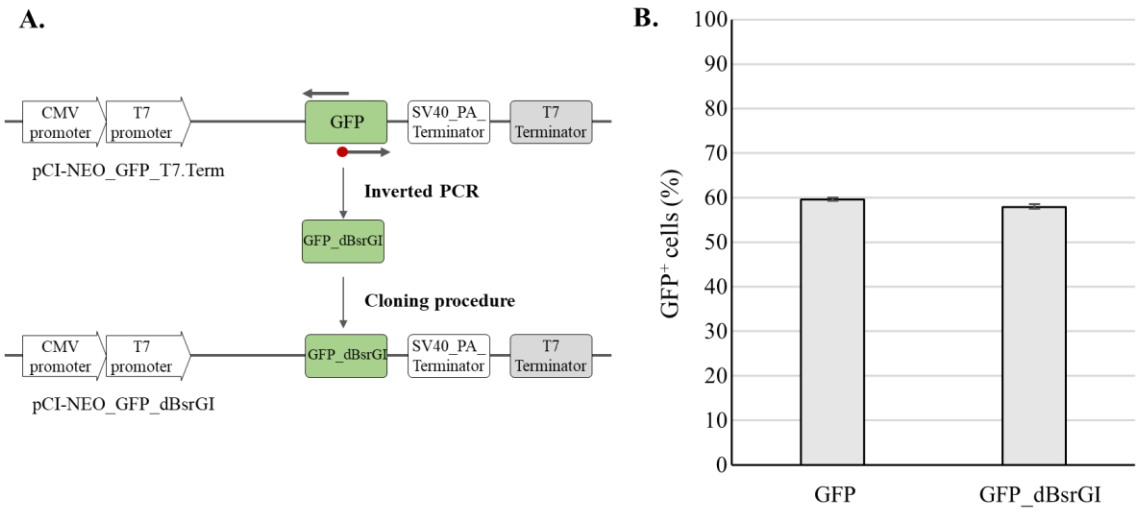

Figure 3.10 – Comparison between GFP and mutated GFP (GFP_dBsrGI). GFP mutated plasmid construction generated through site directed mutagenesis (A), starting with pCI-NEO_GFP_T7.Term, where 5'-phosphorylated primers placed in opposite directions performed an inverted PCR, containing the point mutation allowing to produce the mutated GFP. This fragment was inserted at pCI-NEO_GFP_T7.Term by T4 DNA ligase into pCI-NEO_GFP_T7.Term. Evaluation of GFP_dBsrGI expression in 293T cell line (B). The original non-mutated GFP is shown as control. The percentage of GFP positive cells was determined by flow cytometry and is shown as average ± standard deviation of three technical replicates.

After establishing the plasmid containing the J6/C replicon tagged with GFP, the DNA template was *in vitro* transcribed to generate the RNA replicon and transfected into Huh-7.5 cells. However, due to major differences in the transcript length between the GFP control (of around 1 kb) and the replicon (of around 10 kb) an additional assay of transfection optimization was conducted. To that end, two ratios of LF:RNA of 1 µL of LF to 333 ng of RNA and 1 µL of LF to 666 ng of RNA, recommended by the supplier, were used. Then 500, 1500, 2500 and 5000 ng of RNA were tested and evaluated at 24 hours post-transfection (Figure 3.11 A). The results showed a very low percentage of GFP positive cells in all conditions (1.8% to 3.2%). The best transfection conditions were those using 1500 ng of RNA at the ratio of 1:333 and 5000 ng of RNA at the ratio of 1:666. For these conditions, GFP translation was repeated and was evaluated at 24, 48 and 72 hours post-transfection (Figure 3.11 B). The results revealed an increase of GFP positive cells over time, demonstrating the tagged replicon functionality. For the condition using 1500 ng of RNA and 1:333 of LF:RNA ratio, the percentage of GFP positive cells at 72 hours post-transfection increased 3-fold when comparing to 24 hours post-transfection, reaching almost 9%. Based on these results, and despite the low levels of GFP positive cells, the ratio of 1: 333 using 1500 ng of RNA at 72 hours post-transfection was selected as the best condition for transfecting the replicon.

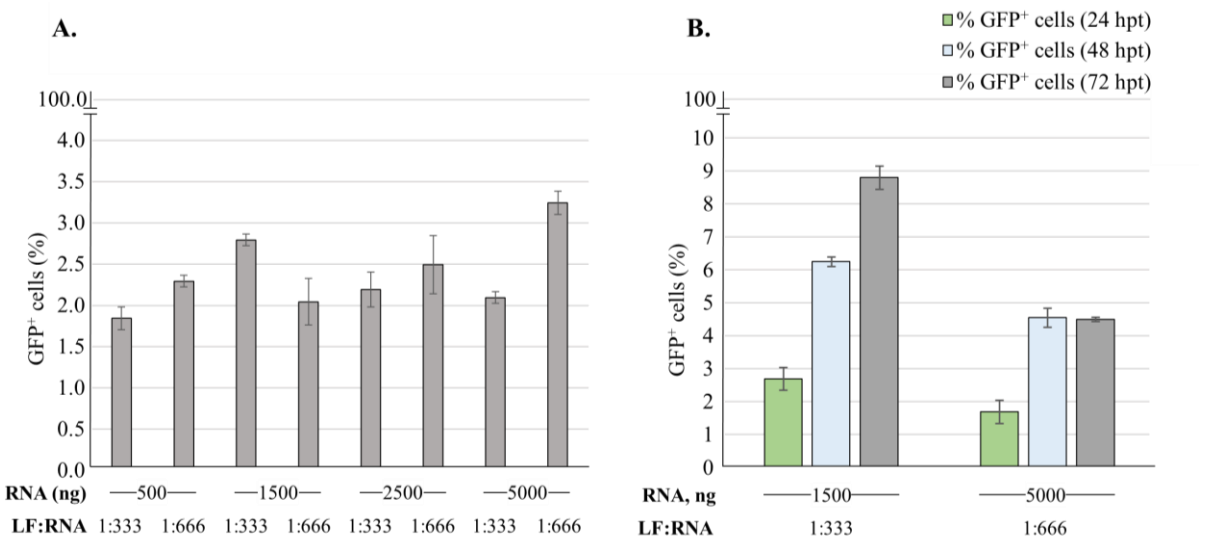

Figure 3.11 – Optimization of J6/C_GFP transfection conditions. J6/C_GFP RNA synthesized *in vitro* was transfected into Huh-7.5 using 500, 1500, 2500 and 5000 ng per well in 24 well plates, using the ratios of 1 µL LF to 333 or 666 ng of RNA and evaluated, at 24 hours post-transfection (A). For the best transfection conditions using 1500 and 5000 ng of RNA and ratios of 1 µL LF to 333 and 1 µL LF to 666 ng of RNA respectively, the transfection was repeated and GFP expression was evaluated at 24, 48 and 72 hours post-transfection (hpt) (B). In both A and B the percentage of GFP positive cells were determined using flow cytometry and values are shown as average ± standard deviation of two technical replicates.

To understand the low percentage of GFP positive cells when transfected with the tagged replicon, the intracellular levels of GFP mRNA were quantified by RT-qPCR (Figure 3.12), the commercial GFP RNA was used as control. The results showed that using commercial GFP RNA resulted in 75-fold higher RNA levels than when using the tagged replicon, J6/C_GFP.

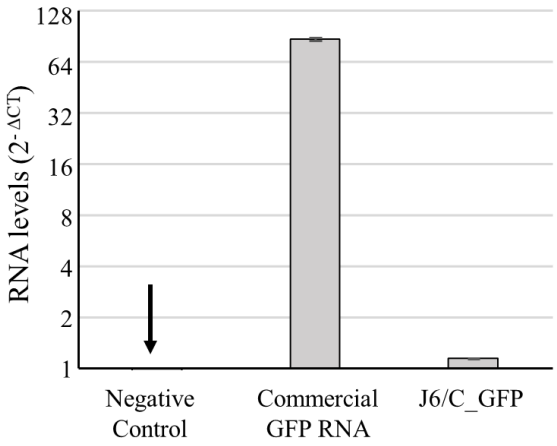

Figure 3.12 - Comparison of intracellular RNA levels when using commercial GFP RNA or *in vitro* synthesized J6/C-GFP replicon. In commercial GFP RNA and J6/C_GFP replicon, transfection was carried out using the best conditions, previously defined: 500 ng of commercial RNA at the ratio of 1 µL of LF to 333 ng of RNA and 1500 ng of J6/C-GFP and the ratio of 1 µL of LF to 333 ng of RNA. The intracellular RNA levels were quantified using the $2^{-\Delta Ct}$ method, and RPL22 as internal reference gene. Results are shown as average ± standard deviation of two technical replicates. Black arrow indicates the absence of RNA levels in negative control which correspond to non-transfected cells.

The low intracellular levels of GFP mRNA were contextualized considering the RNA copy number of commercial GFP or the tagged replicon per mass basis (Table 3.5), using the following equation:

$$\text{ssRNA copy number} = \frac{\text{mass of ssRNA g x 6.022e23 molecules/mol}}{\text{number of ribonucleotide of ssRNA x 321.47 g/mol} + 18.02\ \text{g/mol}}$$

(Formula from NEB calculator - https://nebiocalculator.neb.com/#!/ssrnaamt accessed: 1th December 2020)

The RNA copy number of the commercial GFP was found to be 13-fold higher than the tagged replicon, since GFP transcript had 1 kb and the tagged replicon had around 10 kb. Moreover, the results obtained in Figure 3.12, when the transfection occurred using 500 ng of GFP transcript and 1500 ng of the tagged replicon, presented a 4-fold higher RNA copy number. However, the intracellular RNA levels were evaluated, this corresponded to a 75-fold difference, which indicated that was a problem of tagged replicon delivery into cells that did not occurred in the commercial GFP.

Table 3.5– Comparison of RNA copy number between commercial GFP and J6/C_GFP.

	RNA (ng)	RNA copy number (10^{10})
GFP	500	120
J6/C_GFP	500	9
	1500	28
	2500	46
	5000	92

3.4. Implementation of a protocol for immunofluorescence-based screening

After demonstrating the functionality of the tagged replicon in Huh-7.5 cells, it had to be validated the HCV protein expression. For that, an immunofluorescence-based assay was chosen. This assay would allow to understand whether the tagged replicon was a good reporter system of HCV competent cells. A primary antibody against NS3 was used to detect the non-structural viral protein, and the steps of cell fixation, permeabilization and immunostaining were implemented and optimized.

We started by optimizing the concentration of the fixation buffer and evaluated the concentrations of 1%, 2% and 4% (v/v) of paraformaldehyde in PBS (Figure 3.13). The results showed that all tested concentrations of fixation buffer enabled an efficient fixation, although in the conditions using 1% and 2% (v/v) of paraformaldehyde, cells suffered a slight decrease in size when compared to non-fixated cells (Figure 3.13 A and B). Therefore, the optimized fixation condition was set at 4% (v/v) of paraformaldehyde. Under these conditions, the fixation protocol allowed to store fixated Huh-7.5 cells at 4 ºC for, at least, one

week. However, flow cytometer results also showed that around 45% of FC events were cells in doublets (Figure 3.13 D to G).

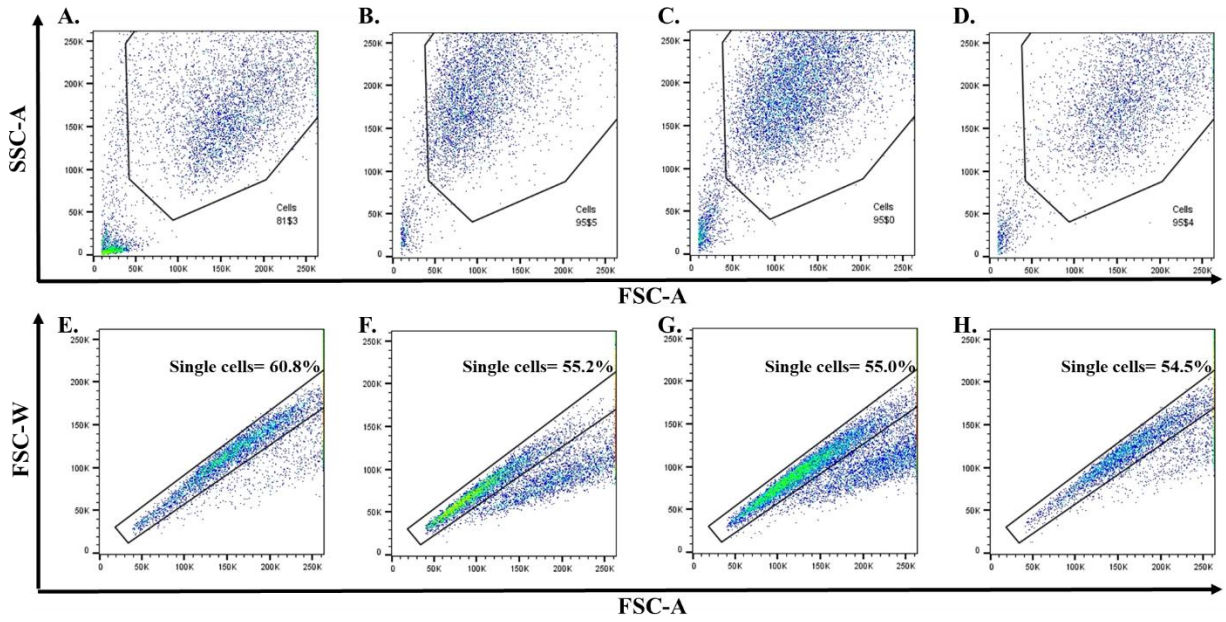

Figure 3.13 - Optimization of fixation buffer concentration. Graphs shows forward versus side scatter (FSC vs SSC) gating to identify cells based on size and granularity (A to D), and forward scatter area versus forward scatter weight (FSC-A vs FSC-W) gating to identify single cells (E to H). Non-fixated cells (A and E) are shown as controls. Cells were fixated using paraformaldehyde at the concentration of 1% (v/v) (B and F), 2% (v/v) (C and G) and 4% (v/v) (D and H). Flow cytometry analyses of cells was performed one week after fixation.

To minimize doublets formation, resuspension was optimized using 10x, 20x and 40x of micropipette resuspension, during the protocol step of fixation (Figure 3.14). The results showed that 10x of micropipette resuspension was the setpoint since a higher percentage of single cells were obtained than previously (Figure 3.13 E to H), and all tested conditions were appropriated to have a single cell suspension.

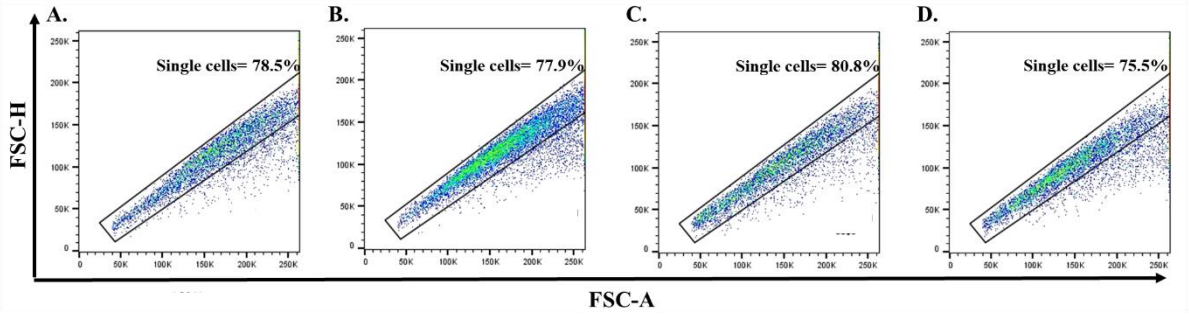

Figure 3.14 - Optimization of resuspension in the fixation step of the immunofluorescence protocol. Non-fixated cells (A), fixated cells resuspended 10x (B), 20x (C) and 40x (D). Graphs show forward scatter area versus forward scatter height (FSC-A vs FSC-H) gating to identify single cells. Flow cytometry analyses of cells was performed one week after fixation.

Before proceeding with the evaluation of the tagged replicon, the validation of the primary antibody against NS3 was assessed. In this antibody validation step, the transfection occurred using J6/C, which is the original replicon and has not been modified, to determinate if the primary antibody is able to detect the

viral protein. Additionally, in the same assay, the concentration of this antibody was optimized, testing three dilutions of 1:20, 1:100 and 1:500. To this end, Huh7-5 cell line were transfected simulating the conditions for the screening of clones, cells were co-transfected with RNA encoding mCherry and J6/C replicon, for the primary antibody optimization and mCherry single-stained condition. For Alexa Fluor 488 secondary antibody single-stained condition, cells were co-transfected with RNA stuffer and J6/C. The stuffer RNA allowed to perform all the transfections under the same total RNA mass condition, it was the GFP transcript (from pCI-NEO_GFP_T7.Term) obtained from IVT without adding ARCA, lacking the mechanism of translation initiation. Hence, this transcript is of the same length of mCherry. The transfected cells were previously fixated and permeabilized under the optimized conditions, at 72 hours post-transfection. The primary antibody was incubated under the optimizing dilutions, and then the staining using Alexa Fluor 488 secondary antibody against the primary antibody was performed. The tested conditions are represented in Table 3.6. Moreover, an experimental control using an isotype control antibody was performed. The isotype antibody lacks specificity to the target and is constituted by the type of the primary antibody (i. e., IgG antibody produced in mouse). This condition allows to distinguish non-specific background caused by secondary antibody, since the isotype primary antibody do not bind to cellular proteins, it is expected a negative signal.

Table 3.6 - Primary antibody validation and opimization assay.

		RNA (1500 ng)	RNA (500 ng)	1º Antibody	2º Antibody
FACS control [a)]	Non-transfected cells	-	-	-	-
	Single-positive mCherry	J6/C	mCherry	Isotype	
	Single-positive Alexa Fluor 488	J6/C	Stuffer *	1:20 NS3	Alexa Fluor 488
Experiment control [b)]	Isotype negative control	J6/C	stuffer	Isotype	Alexa Fluor 488
	Transfection positive control	J6/C	mCherry	-	-
Primary antibody optimization [c)]	Double-transfection	J6/C	mCherry	1:20 NS3	Alexa Fluor 488
	Double-transfection	J6/C	mCherry	1:100 NS3	Alexa Fluor 488
	Double-transfection	J6/C	mCherry	1:500 NS3	Alexa Fluor 488

a) FACS control: flow cytometry controls, includes a double negative control (non-transfected and unstained cells); and a single positive for each fluorochrome (mCherry and Alexa Fluor 488 secondary antibody).
b) Experiment controls: include antibody negative control, using an isotype of the primary antibody; the transfection positive control, using mCherry.
c) Optimization: Antibody anti-NS3 optimization, testing the dilution of 1:20, 1:100 and 1:500.
*** Stuffer:** is the GFP transcript from pCI-NEO_GFP_T7.Term without any mechanism of translation initiation.

The results of validation and optimization revealed that the secondary antibody led to unspecific staining, since the conditions using Alexa Fluor 488 secondary antibody presented above 90% of positive cells (Figure 3.15 C, D, F, G and H). Or, the isotype primary antibody was detecting a intracellular protein, therefore generating a positive signal, of 97% (Figure 3.15 D). Therefore, none of the results obtained could be considered valid.

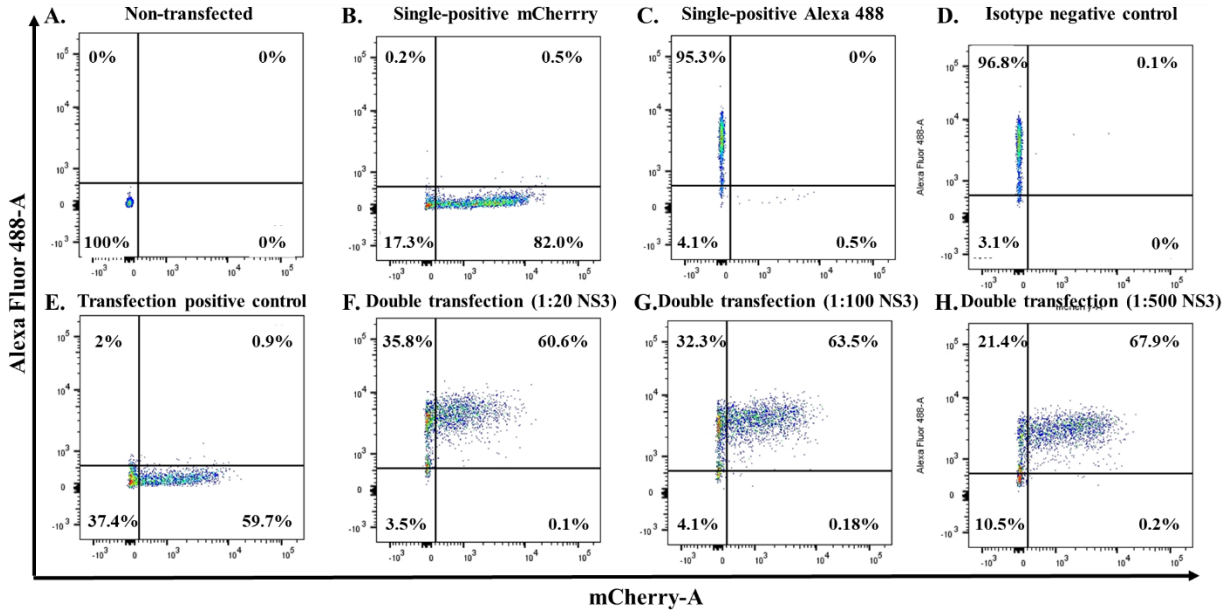

Figure 3.15 – Optimization of the staining conditions of the immunofluorescence protocol, for replicon detection. Graphs show flow cytometry results, graphs shown mCherry intensity area versus Alexa 488 intensity area (mCherry-A vs Alexa Fluor 488-A) gating to allow the identification of mCherry or Alexa Fluor 488 single-positive cells, and double-positive cells. The assay controls were: double-negative control, corresponding to non-stained cells (A); mCherry single positive, transfected with commercial mCherry RNA, stained with isotype (B); Alexa Fluor 488 single positive transfected with the stuffer and J6/C (untagged replicon), and stained with 1:20 anti-NS3 antibody (C); the isotype control, transfected with the stuffer and J6/C (untagged replicon), and stained with the primary antibody isotype (D). For the primary antibody concentration optimization, cells where transfected with the commercial mCherry and J6/C, and stained with the primary antibody anti-NS3 at 1:20 (F), 1:100 (G) and 1:500 (H).

Previous result showed that the Alexa Fluor 488 secondary antibody presented an unspecific staining, which can be the result of non-optimized concentration, or due to isotype primary antibody linked to a cell protein. As a result, the negative controls, with and without isotype primary antibody, under two concentrations of the secondary antibody were tested (Table 3.7). The results showed a percentage of Alexa Fluor 488 positive cells above 90% in all tested conditions, showing the problem of the positive signal was due to an unspecific staining of secondary antibody. Therefore, the secondary antibody usage under these fixation and permeabilization conditions was not possible.

Table 3.7 – Evaluation of Alexa Fluor 488 secondary antibody.

	Alexa Fluor 488 secondary antibody (dilution)*	Alexa Fluor 488 secondary antibody^{+} cells (%)
Negative isotype control	1:100	99.1
	1:500	90.0
Isotype control	1:100	98.8
	1:500	93.7

* Alexa Fluor 488 secondary antibody dilution tested at the dilution of 1:100 and 1:500.

4. DISCUSSION AND CONCLUSIONS

Hepatocytes are targeted by several hepatotropic pathogens, for which effective therapeutic or prophylactic solutions are still missing. Among these pathogens, HCV represents a main contributor for chronic liver disease leading to almost half a million deaths per year[7,10]. To reduce the spreading and reduce new HCV infections, the development of a vaccine is essential. An important limitation to develop the HCV vaccine is the lack of research and development tools, including competent *in vitro* hepatic cell culture systems or suitable animal models[107] for HCV infection. To increase the availability of better *in vitro* hepatic cell culture systems to serve this field, the research project where this thesis was developed, aims to established new hepatic cell lines highly competent and permissive to HCVwt infection, replication, and viral particles production.

These new cell lines are being established by an advanced immortalization strategy, where several immortalizing genes and adjuvant microRNAs are randomly combined. This approach ultimately results in hundreds of immortalized cell clones with different properties and, expectably, different ability to support HCV replication and particles assembly. Therefore, in the context of this thesis, a new molecular tool and protocols to enable fast and high-throughput screening of these clones were established. This tool was tagged full-length HCV replicon based on J6/C tagged with a GFP reporter, allowing to distinguish HCV replicative from non-replicative clones, through a fluorescent signal.

The delivery of replicons to the host cells are common in RNA virology studies[108], and is essential in the HCV field. It is usually perform by electroporation[108,109], given that the RNA molecule size renders alternative delivery vehicles less efficient. Even though electroporation is widely used, it has disadvantages, such as hampering the throughput of RNA delivery to cells, which makes rapid cloning screening unfeasible. Hence, in this work we considered the use of lipofectamine as an alternative to electroporation, to achieve higher throughput in screening of the clones. Lipofection is known to be efficient and it is the "gold-standard" transfection reagent in DNA and RNA delivery even in difficult cells to transfect[110,111]. Hence, this thesis started by optimizing the delivery of RNA molecules to Huh-7.5 cells using a particular formulation of lipofectamine optimized for the delivery of mRNA (Figure 3.1). Lipofection showed to be efficient at delivering commercial GFP RNA in all condition tested, especially for the condition using 500 ng of RNA at the ratio of 1 µL of LF to 333 ng of RNA, which was thus set as the best condition for the following studies. The results also suggested a cytotoxic effect in cells when lipofectamine was present in higher concentrations, due to an increase of cell death (Figure 3.1), this effect precludes the delivery of higher concentrations of RNA, which was a drawback in this work. This effect is caused by the entry of the lipoplexes (complexes of lipotransfection reagent and nucleic acids), which causes disturbances to cell at a mitoses and cytoplasm level, and is a common consequence of the chemical transfection[112].

Although the use of lipofectamine was suitable to transfect the GFP transcripts, we soon realized that the optimizing transfection conditions for the replicon had to be further optimized (Figure 3.11). In this context, transfection efficiency of the tagged replicon was low in all tested conditions, and optimized when using the concentration of 1500 ng of RNA (Figure 3.11 A). The differences of the results between the transfection of control transcripts and the tagged replicon may be explained by the major differences between their length, transfection using 500 ng of GFP transcripts RNA corresponds to 4-fold higher RNA copy number than using 1500 ng of tagged replicon RNA (Table 3.5). Reaching the same RNA copy number of tagged replicon as the reporter transcripts, during transfection, was not possible, because of the major cytotoxic effects caused by the high lipofectamine concentration usage. The much higher length of the replicon may difficult the formation of lipidic-RNA complexes, leading to a different delivery capacity of the RNA molecules when comparing the transfection efficiency of the GFP transcript and that of the replicon. When analyzed the intracellular RNA levels, the difference of 4-fold in RNA copy number during transfections, corresponded to a difference of 75-fold at a cellular level (Figure 3.12). The lower level of intracellular RNA supports this hypothesis of a delivery problem in lipofection when using high length transcripts, which can be caused by the adsorption of the molecules by the cationic-lipid. The adsorption is determined by the RNA weight and charge density, in high molecular wight RNAs (as the replicon) the probability of detaching molecules is high[113]. Despite the low transfection efficiency, cells transfected with the tagged replicon exhibited an increase of GFP signal over time (Figure 3.11 B), confirming that the replicon was functional. Therefore, one of the main aims of this thesis was achieved. Furthermore, a lower expression of full-length replicon when compared with the tagged subgenomic replicon reported in [72] is expected, since the replication efficiency of full-length replicons is lower when comparing to subgenomic replicons[114].

Another major achievement of this thesis was the implementation of an *in vitro* transcription protocol (Figure 3.2), allowing the production of the RNA transcripts, including HCV replicons. Overall, the synthesized RNA molecules presented high yields and purity (Table 3.1), and a good integrity (Figure 3.3). The synthesized transcripts yields were slightly different, which can be explained by the different T7 polymerase behavior in each RNA. This behavior may produce heterogenies transcripts when transcription terminate earlier and do not reach the 3´end[115], producing more abortive shorter sequences[116]. Furthermore, variability between *in vitro* synthesized transcripts was low, showing that the protocol was robust and reproducible (Table 3.3). The implementation of this protocol was of major value considering that was missing in the laboratory.

The establishment of a plasmid containing a reporter gene (Figure 3.4 A) was crucial to establish and validate the *in vitro* transcription protocol. We also considered using transcripts produced with a similar

construction (containing mCherry instead of GFP, Figure 3.4 B) as co-transfection control for the final setting of clone screening. The translation initiation of the reporter gene was tested under the cap-dependent mechanism, however, a cost analysis (Table 3.4), together with the transfection performance of these transcripts (Figure 3.5) led us to choose the commercial mCherry RNA as a control, when we reach to that stage. The cap structure added to the transcript, during IVT reaction, showed to be essential for its translation in the cytoplasm, otherwise transcript lack a mechanism to recruit the translation machinery, and therefore the protein is not synthesized[117]. Although the cap structure allowed the translation of the reporter gene, it never reached the efficiency obtained with the commercial RNA. In fact, the analysis of intracellular GFP RNA levels revealed higher levels in commercial GFP (Figure 3.6), even though the mass of transfected RNA were the same. These results are aligned with a potential lower stability or the increased susceptibility to degradation of the transcripts generated by IVT relative to the commercial alternative. Lower stability or increased susceptibility to degradation could be expected since the IVT transcripts may stimulate the cellular immune system due to the presence of double-stranded RNA caused by the complementary of the transcript with an antisense RNA synthesized through a promotor-less transcription initiation[118], or by the folding dynamic of the molecule, which can leads to multiple intra-molecular or inter-molecular interactions[115]. Overall, the usage of ARCA to synthesized internal control transcripts was disregarded. However, the work conducted on the optimization of this cap analog will be very useful for other applications requiring *in vitro* synthesized transcripts, especially for the cases where commercial RNAs are not available.

In another attempt to establish an internal control and avoid the use of commercial RNA, we constructed a set of plasmids delivering transcripts with an alternative translation initiation mechanism independent of cap. The transcript translation initiation was mediated by IRES structures (Figure 3.7). The choice of the IRES is a critical factor for translation since its efficiency is dependent on the activity each IRES exhibits intracellularly. The activity from three class-assigned IRES and one IRES-like region were evaluated, but only two allowed a successful GFP translation initiation: those of EMCV and PV (Figure 3.8). The type II IRES from EMCV presented the highest translation efficiency and it is, indeed, a popular RNA element widely used for a high level of cap-independent protein translation RNAs[119]. In this context, PV IRES functionality was demonstrated in Huh-7.5 cell line, even though the virus present a neurotropism[120,121]. On the other hand, the IRES from HCV and HIV-1 did not support protein translation. In the case of HCV IRES, we later found that it is essential to include a part of the core protein to achieve efficient HCV IRES translation[122,123]. This part was not included in our construction and may explain the absence of protein expression. In the case of the RNA of HIV-1, the translation initiation usually occurs in a cap-dependent mechanism. But, when cells are expose to certain conditions, such as stress, a switch takes place and translation starts to be mediated by the IRES-like region[124]. This may explain the absence of translation in transcript delivered by HIV-1 IRES. The IRES usage in the internal control transcript did not

suit the purpose since it presents a lower performance than commercial RNAs. Additionally, the IRES strength can be influenced by the host and viral factors[125,126], which preclude its use because the expression of internal control can not vary between clones. This work allowed a comparison side-by-side of the IRES activity (to be completed with the HAV IRES).

HCV replicons allow the study of the virus *in vitro* since they are able to replicate in permissive cells. The full-length replicon J6/C presents a higher replication and allows the production of HCVcc with higher titers[71] when comparing to other replicons. Therefore, in this thesis, we established a reporter replicon based on J6/C tagged with a GFP fused at the NS5A (Figure 3.9) and, this site was chosen because it was successfully used previously in a subgenomic replicon[72]. The GFP tagged replicon allows the identification of cells capable of replicating the virus in a quantitative approach, i. e., the more the intensity of the GFP signal, the highest the replication rate. Moreover, the HCVcc particles can be harvest, quantified, and assessed for their infectivity. This adds a second layer of information on the functionality of each cell clone in supporting the completion of the virus life cycle.

Transfecting the tagged replicon into Huh-7.5 cells resulted in GFP-expressing cells (Figure 3.11 A). Although at low levels, most likely duo to size constraints as discussed previously, the increase in GFP signal along time also supported the functionality of its replication capacity (Figure 3.11 B). However, it was still missing the evaluation and validation on whether the GFP signal was a direct reporter on the expression of HCV proteins. This last evaluation assay was conducted based on an immunofluorescence protocol. In the first step of this protocol, it was proceeded a fixation optimization. Fixated cells maintained size and granularity characteristics similar to non-fixated cells in the condition using 4% of fixation buffer (Figure 3.13), as expected, since usually the fixation of live mammalian cells is perform under this concentration of paraformaldehyde[127], allowing a correct crosslinking of the molecules[128]. Noteworthy, the suspension of fixed cells revealed a high percentage of aggregates, thereby, resuspension in the fixation step was evaluated (Figure 3.14), but no differences were found, which means that the setpoint to avoid the aggregates formation was below of ten times resuspension.

After having implemented and determined the fixation and permeabilization steps of the protocol, the validation and optimization of the primary antibody against NS3 was performed. Due to time constrains, an experimental design that covered the various aspects necessary for validation was carried out (Table 3.6). However, the negative isotype control reported a positive signal (Figure 3.15), with nearly 100% of stained cells when no positive cells were expected. Further analysis (Table 3.7) revealed that the unspecificity comes from the secondary antibody. Therefore, a new experimental assay, more stepwise, is required for the antibody validation.

In this Master thesis we established and validate a new molecular tool, for screening of HCV permissive cells, and implemented a set of protocols applied to handle and produce HCV, including an *in vitro* transcription protocol for RNA synthesis. Throughout the thesis, the cap-dependent and cap-independent mechanisms of translation initiation were explored in the context of generating internal reporter controls. Further work is required until reaching the stage of screening the new clones generated by immortalization to identify those cells highly permissive to HCV replication. These new cells can be used to better serve HCV research field, but also to study other hepatotropic pathogens, such as the parasite protozoan *Plasmodium* family leading to development of malaria [6,129].

5. FUTURE WORK

The work developed during this master thesis contributed to a better screening methodology for cell lines permissive to HCV infection. To achieve this final stage, the work started herein will continue to be developed.

First, the delivery mechanism of the tagged replicon will be optimized to overcome the problem of low transfection efficiency. Therefore, the clone screening based on electroporation delivery will be performed, although with a reduced throughput and a more intensive manual work to proceed. We expect a higher GFP expression from the tagged replicon than reported when using lipofectamine, after this optimization, the following validations will be performed.

The validation of the primary antibody against NS3 was not concluded due to unspecific staining of the Alexa Fluor 488 secondary antibody. Since this reagent has been previously used and shown to enable specific staining, we suspect of the particular fixation and permeabilization protocol used in this thesis. Therefore, to understand this lack of specificity, the Alexa Fluor 488 secondary antibody immunostaining will be tested in fixated and non-fixated cells, and in permeabilized and non- permeabilized cells. In parallel, an immunostaining protocol in coverslips using an alternative fixative (methanol) will also be carried out for the purpose of validating solely the primary antibody. Having an immunofluorescence assay that enables assessing the purpose of detect the J6/C viral proteins is essential to validate the reporting capacity of the tagged replicon created in this work.

Specifically, the tagged replicon will be validated using an experimental design similar to that described in Table 3.6, but using Alexa Fluor 594 secondary antibody (red). We expect to see GFP positive cells, where the tagged replicon is reporting its activity, corresponding to the red-stained cells, where is identified the viral protein NS3.

Following the optimization of the delivery and validation of the reporter capacity of the tagged replicon, the final step of screening PHH immortalized clones will be performed. Clones will be co-transfected with the GFP tagged replicon and a mCherry commercial transcript. The latter functions as an internal control to account for transfection efficiency, which can be different across clones. Hence, it is essential that the tagged replicon signal is normalized to this level. GFP positive clones will be cells permissive to HCV replicon. Moreover, the GFP intensity normalized to the transfection efficiency provide quantitative grading on the efficiency of the clone for HCV replication, allowing to select the highly permissive cells. Additionally, for each GFP positive clone, the supernatant will be harvested to quantify the titer of HCVcc and evaluate and tested their infectious capacity.

6. BIBLIOGRAPHY

1. Bhatia SN, Underhill GH, Zaret KS, Fox IJ. Cell and tissue engineering for liver disease. *Sci Transl Med*. 2014. doi:10.1126/scitranslmed.3005975

2. Thomson AW, Knolle PA. Antigen-presenting cell function in the tolerogenic liver environment. *Nat Rev Immunol*. 2010. doi:10.1038/nri2858

3. Horst AK, Neumann K, Diehl L, Tiegs G. Modulation of liver tolerance by conventional and nonconventional antigen-presenting cells and regulatory immune cells. *Cell Mol Immunol*. 2016. doi:10.1038/cmi.2015.112

4. Zhou Z, Xu MJ, Gao B. Hepatocytes: A key cell type for innate immunity. *Cell Mol Immunol*. 2016. doi:10.1038/cmi.2015.97

5. Gural N, Mancio-Silva L, He J, Bhatia SN. Engineered Livers for Infectious Diseases. *CMGH*. 2018. doi:10.1016/j.jcmgh.2017.11.005

6. WHO. *Guidelines for the Care and Treatment of Persons Diagnosed with Chronic Hepatitis C Virus Infection*.; 2018.

7. Hollande C, Parlati L, Pol S. Micro-elimination of hepatitis C virus. *Liver Int*. 2020;40(S1):67-71. doi:10.1111/liv.14363

8. Catanese MT, Dorner M. Advances in experimental systems to study hepatitis C virus in vitro and in vivo. *Virology*. 2015;479-480:221-233. doi:10.1016/j.virol.2015.03.014

9. Scheel TKH, Rice CM. Understanding the hepatitis C virus life cycle paves the way for highly effective therapies. *Nat Med*. 2013. doi:10.1038/nm.3248

10. Bukh J. The history of hepatitis C virus (HCV): Basic research reveals unique features in phylogeny, evolution and the viral life cycle with new perspectives for epidemic control. *J Hepatol*. 2016;65(1):S2-S21. doi:10.1016/j.jhep.2016.07.035

11. Waheed Y, Siddiq M, Jamil Z, Najmi MH. Hepatitis elimination by 2030: Progress and challenges. *World J Gastroenterol*. 2018. doi:10.3748/wjg.v24.i44.4959

12. Crouchet E, Wrensch F, Schuster C, Zeisel MB, Baumert TF. Host-targeting therapies for hepatitis C virus infection: current developments and future applications. *Therap Adv Gastroenterol*. 2018. doi:10.1177/1756284818759483

13. Alazard-Dany N, Denolly S, Boson B, Cosset FL. Overview of hcv life cycle with a special focus on current and possible future antiviral targets. *Viruses*. 2019. doi:10.3390/v11010030

14. Ireland G, Mandal S, Hickman M, Ramsay M, Harris R, Simmons R. Mortality rates among individuals diagnosed with hepatitis c virus (HCV): An observational cohort study, England, 2008 to 2016. *Eurosurveillance*. 2019. doi:10.2807/1560-7917.ES.2019.24.30.1800695

15. Wyles DL, Luetkemeyer AF. Understanding hepatitis C virus drug resistance: clinical implications for current and future regimens. *Top Antivir Med*. 2017.

16. Bagaglio S, Uberti-Foppa C, Morsica G. Resistance Mechanisms in Hepatitis C Virus: implications for Direct-Acting Antiviral Use. *Drugs*. 2017. doi:10.1007/s40265-017-0753-x

17. Bailey JR, Barnes E, Cox AL. Approaches, Progress, and Challenges to Hepatitis C Vaccine Development. *Gastroenterology*. 2019. doi:10.1053/j.gastro.2018.08.060

18. Kato T, Date T, Miyamoto M, et al. Efficient Replication of the Genotype 2a Hepatitis C Virus Subgenomic Replicon. *Gastroenterology*. 2003;125(6):1808-1817. doi:10.1053/j.gastro.2003.09.023

19. Rybalko SL, Porva YI, Alekseenko IP, et al. Replication of hepatitis C virus in cell culture. *Biopolym Cell*. 2009;25(1):1-6. doi:10.7124/bc.0007C9

20. Schmitt M, Scrima N, Radujkovic D, et al. A Comprehensive Structure-Function Comparison of Hepatitis C Virus Strain JFH1 and J6 Polymerases Reveals a Key Residue Stimulating Replication in Cell Culture across Genotypes. *J Virol*. 2011;85(6):2565-2581. doi:10.1128/jvi.02177-10

21. Smith DB, Bukh J, Kuiken C, et al. Expanded classification of hepatitis C virus into 7 genotypes and 67 subtypes: Updated criteria and genotype assignment web resource. *Hepatology*. 2014;59(1):318-327. doi:10.1002/hep.26744

22. Steinmann E, Pietschmann T. *Hepatitis C Virus: From Molecular Virology to Antiviral Therapy*. Vol 369.; 2013. doi:10.1007/978-3-642-27340-7

23. Pietschmann T. In sero veritas: What serum markers teach us about HCV infection of primary human hepatocytes. *Gut*. 2014. doi:10.1136/gutjnl-2013-306111

24. Lohmann V, Körner F, Koch JO, Herian U, Theilmann L, Bartenschlager R. Replication of subgenomic hepatitis C virus RNAs in a hepatoma cell line. *Science (80-)*. 1999;285(5424):110-113. doi:10.1126/science.285.5424.110

25. Moradpour D, Penin F. Hepatitis C virus proteins: From structure to function. *Curr Top Microbiol Immunol*. 2013. doi:10.1007/978-3-642-27340-7-5

26. Anjum S, Ali S, Ahmad T, et al. Sequence and structural analysis of 3′ untranslated region of hepatitis C virus, genotype 3a, from Pakistani isolates. *Hepat Mon*. 2013. doi:10.5812/hepatmon.8390

27. Strosberg AD, Kota S, Takahashi V, Snyder JK, Mousseau G. Core as a novel viral target for hepatitis C drugs. *Viruses*. 2010. doi:10.3390/v2081734

28. Gawlik K, Gallay PA. HCV core protein and virus assembly: what we know without structures. *Immunol Res*. 2014. doi:10.1007/s12026-014-8494-3

29. Ouyang B, Xie S, Berardi MJ, et al. Unusual architecture of the p7 channel from hepatitis C virus. *Nature*. 2013. doi:10.1038/nature12283

30. Lorenz IC, Marcotrigiano J, Dentzer TG, Rice CM. Structure of the catalytic domain of the hepatitis C virus NS2-3 protease. *Nature*. 2006. doi:10.1038/nature04975

31. Jirasko V, Montserret R, Appel N, et al. Structural and functional characterization of nonstructural protein 2 for its role in hepatitis C virus assembly. *J Biol Chem*. 2008. doi:10.1074/jbc.M803981200

32. Lin C, Wu JW, Hsiao K, Su MS. The hepatitis C virus NS4A protein: interactions with the NS4B and NS5A proteins. *J Virol*. 1997. doi:10.1128/jvi.71.9.6465-6471.1997

33. Brass V, Berke JM, Montserret R, Blum HE, Penin F, Moradpour D. Structural determinants for membrane association and dynamic organization of the hepatitis C virus NS3-4A complex. *Proc Natl Acad Sci U S A*. 2008. doi:10.1073/pnas.0807298105

34. Gouttenoire J, Penin F, Moradpour D. Hepatitis C virus nonstructural protein 4B: A journey into unexplored territory. *Rev Med Virol*. 2010. doi:10.1002/rmv.640

35. Esser-Nobis K, Romero-Brey I, Ganten TM, et al. Analysis of hepatitis C virus resistance to silibinin in vitro and in vivo points to a novel mechanism involving nonstructural protein 4B. *Hepatology*. 2013. doi:10.1002/hep.26260

36. Sklan EH, Glenn JS. *HCV NS4B: From Obscurity to Central Stage*.; 2006.

37. Zayas M, Long G, Madan V, Bartenschlager R. Coordination of Hepatitis C Virus Assembly by Distinct Regulatory Regions in Nonstructural Protein 5A. *PLoS Pathog*. 2016. doi:10.1371/journal.ppat.1005376

38. Sierra H, Cordova M, Chen CSJ, Rajadhyaksha M. Confocal imaging-guided laser ablation of basal cell carcinomas: An ex vivo study. *J Invest Dermatol*. 2015;135(2):612-615. doi:10.1038/jid.2014.371

39. Kim CW, Chang KM. Hepatitis C virus: virology and life cycle. *Clin Mol Hepatol*. 2013. doi:10.3350/cmh.2013.19.1.17

40. Dustin LB, Bartolini B, Capobianchi MR, Pistello M. Hepatitis C virus: life cycle in cells, infection and host response, and analysis of molecular markers influencing the outcome of infection and response to therapy. *Clin Microbiol Infect*. 2016. doi:10.1016/j.cmi.2016.08.025

41. Moradpour D, Penin F, Rice CM. Replication of hepatitis C virus. *Nat Rev Microbiol*. 2007. doi:10.1038/nrmicro1645

42. Kazakov T, Yang F, Ramanathan HN, Kohlway A, Diamond MS, Lindenbach BD. Hepatitis C Virus RNA Replication Depends on Specific Cis- and Trans-Acting Activities of Viral Nonstructural Proteins. *PLoS Pathog*. 2015. doi:10.1371/journal.ppat.1004817

43. Bartenschlager R, Lohmann V, Penin F. The molecular and structural basis of advanced antiviral therapy for hepatitis C virus infection. *Nat Rev Microbiol*. 2013. doi:10.1038/nrmicro3046

44. Lohmann V. Hepatitis C Virus RNA Replication. In: ; 2013. doi:10.1007/978-3-642-27340-7_7

45. Crouchet E, Baumert TF, Schuster C. Hepatitis C virus–apolipoprotein interactions: molecular mechanisms and clinical impact. *Expert Rev Proteomics*. 2017. doi:10.1080/14789450.2017.1344102

46. Felmlee DJ, Hafirassou ML, Lefevre M, Baumert TF, Schuster C. Hepatitis C virus, cholesterol and lipoproteins - Impact for the viral life cycle and pathogenesis of liver disease. *Viruses*. 2013. doi:10.3390/v5051292

47. Corless L, Crump CM, Griffin SDC, Harris M. Vps4 and the ESCRT-III complex are required for the release of infectious Hepatitis C virus particles. *J Gen Virol*. 2010. doi:10.1099/vir.0.017285-0

48. Jones DM, McLauchlan J. Hepatitis C virus: Assembly and release of virus particles. *J Biol Chem*. 2010. doi:10.1074/jbc.R110.133017

49. Lindenbach BD. Virion assembly and release. *Curr Top Microbiol Immunol*. 2013. doi:10.1007/978-3-642-27340-7-8

50. Lange CM, Jacobson IM, Rice CM, Zeuzem S. Emerging therapies for the treatment of hepatitis C.

EMBO Mol Med. 2014. doi:10.1002/emmm.201303131

51. Bartenschlager R, Pietschmann T. Efficient hepatitis C virus cell culture system: What a difference the host cell makes. *Proc Natl Acad Sci U S A*. 2005;102(28):9739-9740. doi:10.1073/pnas.0504296102

52. Steinmann E, Pietschmann T. Cell Culture Systems for Hepatitis C Virus. In: ; 2013. doi:10.1007/978-3-642-27340-7_2

53. Bukh J, Pietschmann T, Lohmann V, et al. Mutations that permit efficient replication of hepatitis C virus RNA in Huh-7 cells prevent productive replication in chimpanzees. *Proc Natl Acad Sci U S A*. 2002. doi:10.1073/pnas.212532699

54. Elaut G, Henkens T, Papeleu P, et al. Molecular Mechanisms Underlying the Dedifferentiation Process of Isolated Hepatocytes and Their Cultures. *Curr Drug Metab*. 2006. doi:10.2174/138920006778017759

55. Zeilinger K, Freyer N, Damm G, Seehofer D, Knöspel F. Cell sources for in vitro human liver cell culture models. *Exp Biol Med*. 2016;241(15). doi:10.1177/1535370216657448

56. Zeilinger K, Freyer N, Damm G, Seehofer D, Knöspel F. Cell sources for in vitro human liver cell culture models. *Exp Biol Med*. 2016;241(15):1684-1698. doi:10.1177/1535370216657448

57. Gondeau C, Briolotti P, Razafy F, et al. In vitro infection of primary human hepatocytes by HCV-positive sera: Insights on a highly relevant model. *Gut*. 2014. doi:10.1136/gutjnl-2013-304623

58. Ramboer E, De Craene B, De Kock J, et al. Strategies for immortalization of primary hepatocytes. *J Hepatol*. 2014. doi:10.1016/j.jhep.2014.05.046

59. Lauschke VM, Vorrink SU, Moro SML, et al. Massive rearrangements of cellular MicroRNA signatures are key drivers of hepatocyte dedifferentiation. *Hepatology*. 2016;64(5):1743-1756. doi:10.1002/hep.28780

60. Ramboer E, Vanhaecke T, Rogiers V, Vinken M. Immortalized human hepatic cell lines for in vitro testing and research purposes. In: *Protocols in In Vitro Hepatocyte Research*. ; 2015. doi:10.1007/978-1-4939-2074-7_4

61. Sainz B, Tencate V, Uprichard SL. Three-dimensional Huh7 cell culture system for the study of Hepatitis C virus infection. *Virol J*. 2009. doi:10.1186/1743-422X-6-103

62. Pihl AF, Offersgaard AF, Mathiesen CK, et al. High density Huh7.5 cell hollow fiber bioreactor

culture for high-yield production of hepatitis C virus and studies of antivirals. *Sci Rep*. 2018. doi:10.1038/s41598-018-35010-5

63. Li SH, Li XF, Zhao H, et al. Development and characterization of the replicon system of Japanese encephalitis live vaccine virus SA14-14-2. *Virol J*. 2013. doi:10.1186/1743-422X-10-64

64. Schott JW, Morgan M, Galla M, Schambach A. Viral and synthetic RNA vector technologies and applications. *Mol Ther*. 2016. doi:10.1038/mt.2016.143

65. Hannemann H. Viral replicons as valuable tools for drug discovery. *Drug Discov Today*. 2020. doi:10.1016/j.drudis.2020.03.010

66. Uprichard SL. Hepatitis C virus experimental model systems and antiviral drug research. *Virol Sin*. 2010. doi:10.1007/s12250-010-3134-0

67. Blight KJ, Kolykhalov AA, Rice CM. Efficient initiation of HCV RNA replication in cell culture. *Science (80-)*. 2000;290(5498):1972-1974. doi:10.1126/science.290.5498.1972

68. Kato T, Date T, Miyamoto M, et al. Efficient Replication of the Genotype 2a Hepatitis C Virus Subgenomic Replicon. *Gastroenterology*. 2003. doi:10.1053/j.gastro.2003.09.023

69. Lindenbach BD, Evans MJ, Syder AJ, et al. Virology: Complete replication of hepatitis C virus in cell culture. *Science (80-)*. 2005. doi:10.1126/science.1114016

70. Pietschmann T, Kaul A, Koutsoudakis G, et al. Construction and characterization of infectious intragenotypic and intergenotypic hepatitis C virus chimeras. *Proc Natl Acad Sci U S A*. 2006;103(19):7408-7413. doi:10.1073/pnas.0504877103

71. Pietschmann T, Kaul A, Koutsoudakis G, et al. Construction and characterization of infectious intragenotypic and intergenotypic hepatitis C virus chimeras. *Proc Natl Acad Sci U S A*. 2006. doi:10.1073/pnas.0504877103

72. Moradpour D, Evans MJ, Gosert R, et al. Insertion of Green Fluorescent Protein into Nonstructural Protein 5A Allows Direct Visualization of Functional Hepatitis C Virus Replication Complexes. *J Virol*. 2004;78(14):7400-7409. doi:10.1128/jvi.78.14.7400-7409.2004

73. Remenyi R, Qi H, Su S, et al. A Comprehensive Functional Map of the Hepatitis C Virus Genome. *MBio*. 2014;5(5):1-10. doi:10.1128/mBio.01469-14.Editor

74. Liu S, Ansari IH, Das SC, Pattnaik AK. Insertion and deletion analyses identify regions of non-structural protein 5A of Hepatitis C virus that are dispensable for viral genome replication. *J Gen*

Virol. 2006. doi:10.1099/vir.0.81407-0

75. Kawamura A, Miyata T. 4.2 Biosensors. *Biomater Nanoarchitectonics*. 2016. doi:10.1016/B978-0-323-37127-8/00010-8

76. Eyre NS, Aloia AL, Joyce MA, Chulanetra M, Tyrrell DL, Beard MR. Sensitive luminescent reporter viruses reveal appreciable release of hepatitis C virus NS5A protein into the extracellular environment. *Virology*. 2017. doi:10.1016/j.virol.2017.04.003

77. Starr DA. 乳鼠心肌提取 HHS Public Access. *Physiol Behav*. 2011;176(1):139-148. doi:10.1016/j.physbeh.2017.03.040

78. Martinez-Salas E, Francisco-Velilla R, Fernandez-Chamorro J, Embarek AM. Insights into structural and mechanistic features of viral IRES elements. *Front Microbiol*. 2018;8(JAN):1-15. doi:10.3389/fmicb.2017.02629

79. Marcotrigiano J, Gingras AC, Sonenberg N, Burley SK. X-ray studies of the messenger RNA 5' cap-binding protein (eIF4E) bound to 7-methyl-GDP. *Nucleic Acids Symp Ser*. 1997.

80. Kapp LD, Lorsch JR. The Molecular Mechanics of Eukaryotic Translation. *Annu Rev Biochem*. 2004. doi:10.1146/annurev.biochem.73.030403.080419

81. Shatkin AJ. Capping of eucaryotic mRNAs. *Cell*. 1976. doi:10.1016/0092-8674(76)90128-8

82. López-Lastra M, Rivas A, Barría MI. Protein synthesis in eukaryotes: The growing biological relevance of cap-independent translation initiation. *Biol Res*. 2005;38(2-3):121-146. doi:10.4067/S0716-97602005000200003

83. Shirokikh NE, Preiss T. Translation initiation by cap-dependent ribosome recruitment: Recent insights and open questions. *Wiley Interdiscip Rev RNA*. 2018. doi:10.1002/wrna.1473

84. Grudzien E, Stepinski J, Jankowska-Anyszka M, Stolarski R, Darzynkiewicz E, Rhoads RE. Novel cap analogs for in vitro synthesis of mRNAs with high translational efficiency. *RNA*. 2004. doi:10.1261/rna.7380904

85. Hegde MR, Crowley MR. Genome and gene structure. In: *Emery and Rimoin's Principles and Practice of Medical Genetics and Genomics: Foundations*. ; 2018. doi:10.1016/B978-0-12-812537-3.00004-4

86. Ramanathan A, Robb GB, Chan SH. mRNA capping: Biological functions and applications. *Nucleic Acids Res*. 2016. doi:10.1093/nar/gkw551

87. Ghosh A, Lima CD. Enzymology of RNA cap synthesis. *Wiley Interdiscip Rev RNA*. 2010. doi:10.1002/wrna.19

88. Fechter P, Brownlee GG. Recognition of mRNA cap structures by viral and cellular proteins. *J Gen Virol*. 2005. doi:10.1099/vir.0.80755-0

89. Kowalska J, Lewdorowicz M, Zuberek J, et al. Synthesis and characterization of mRNA cap analogs containing phosphorothioate substitutions that bind tightly to eIF4E and are resistant to the decapping pyrophosphatase DcpS. *RNA*. 2008. doi:10.1261/rna.990208

90. Mokrejs M. IRESite: the database of experimentally verified IRES structures (www.iresite.org). *Nucleic Acids Res*. 2006;34(90001):D125-D130. doi:10.1093/nar/gkj081

91. Willcocks MM, Zaini S, Chamond N, et al. Distinct roles for the IIId2 sub-domain in pestivirus and picornavirus internal ribosome entry sites. *Nucleic Acids Res*. 2017. doi:10.1093/nar/gkx991

92. Lozano G, Francisco-Velilla R, Martinez-Salas E. Deconstructing internal ribosome entry site elements: An update of structural motifs and functional divergences. *Open Biol*. 2018. doi:10.1098/rsob.180155

93. Komar AA, Hatzoglou M. Cellular IRES-mediated translation: The war of ITAFs in pathophysiological states. *Cell Cycle*. 2011. doi:10.4161/cc.10.2.14472

94. Gritsenko AA, Weingarten-Gabbay S, Elias-Kirma S, Nir R, de Ridder D, Segal E. Sequence features of viral and human Internal Ribosome Entry Sites predictive of their activity. *PLoS Comput Biol*. 2017. doi:10.1371/journal.pcbi.1005734

95. Mailliot J, Martin F. Viral internal ribosomal entry sites: four classes for one goal. *Wiley Interdiscip Rev RNA*. 2018. doi:10.1002/wrna.1458

96. Sweeney TR, Dhote V, Yu Y, Hellen CUT. A Distinct Class of Internal Ribosomal Entry Site in Members of the Kobuvirus and Proposed Salivirus and Paraturdivirus Genera of the Picornaviridae. *J Virol*. 2012. doi:10.1128/jvi.05862-11

97. Asnani M, Kumar P, Hellen CUT. Widespread distribution and structural diversity of Type IV IRESs in members of Picornaviridae. *Virology*. 2015. doi:10.1016/j.virol.2015.02.016

98. Hashem Y, Des Georges A, Dhote V, et al. Hepatitis-C-virus-like internal ribosome entry sites displace eIF3 to gain access to the 40S subunit. *Nature*. 2013. doi:10.1038/nature12658

99. Jaafar ZA, Oguro A, Nakamura Y, Kieft JS. Translation initiation by the hepatitis C virus IRES

requires eIF1A and ribosomal complex remodeling. *Elife*. 2016;5(DECEMBER2016):1-23. doi:10.7554/eLife.21198

100. Shi ST, Lai MMC. HCV 5′ and 3′UTR: When Translation Meets Replication. *Hepat C Viruses Genomes Mol Biol*. 2006:49-87. http://www.ncbi.nlm.nih.gov/pubmed/21250387.

101. Weiner MP, Costa GL, Schoettlin W, Cline J, Mathur E, Bauer JC. Site-directed mutagenesis of double-stranded chain reaction DNA by the polymerase. 1994;151:119-123.

102. Blight KJ, McKeating JA, Rice CM. Highly Permissive Cell Lines for Subgenomic and Genomic Hepatitis C Virus RNA Replication. *J Virol*. 2002;76(24):13001-13014. doi:10.1128/jvi.76.24.13001-13014.2002

103. Nakabayashi H, Miyano K, Sato J, Yamane T, Taketa K. Growth of human hepatoma cell lines with differentiated functions in chemically defined medium. *Cancer Res*. 1982;42(9):3858-3863.

104. Graham FL, Smiley J, Russell WC, Nairn R. Characteristics of a human cell line transformed by DNA from human adenovirus type 5. *J Gen Virol*. 1977. doi:10.1099/0022-1317-36-1-59

105. DuBridge RB, Tang P, Hsia HC, Leong PM, Miller JH, Calos MP. Analysis of mutation in human cells by using an Epstein-Barr virus shuttle system. *Mol Cell Biol*. 1987. doi:10.1128/mcb.7.1.379

106. Livak KJ, Schmittgen TD. Analysis of Relative Gene Expression Data Using Real- Time Quantitative PCR and the 2 ‘ □□ C T Method. 2001;408:402-408. doi:10.1006/meth.2001.1262

107. Duncan JD, Urbanowicz RA, Tarr AW, Ball JK. Hepatitis C virus vaccine: Challenges and prospects. *Vaccines*. 2020. doi:10.3390/vaccines8010090

108. Gonzalez G, Pfannes L, Brazas R, Striker R. Selection of an optimal RNA transfection reagent and comparison to electroporation for the delivery of viral RNA. *J Virol Methods*. 2007. doi:10.1016/j.jviromet.2007.04.013

109. Hashemi A, Roohvand F, Ghahremani MH, et al. Optimization of transfection methods for Huh-7 and Vero cells: A comparative study. *Cytol Genet*. 2012. doi:10.3103/S0095452712060035

110. Cardarelli F, Digiacomo L, Marchini C, et al. The intracellular trafficking mechanism of Lipofectamine-based transfection reagents and its implication for gene delivery. *Sci Rep*. 2016. doi:10.1038/srep25879

111. Zou S, Scarfo K, Nantz MH, Hecker JG. Lipid-mediated delivery of RNA is more efficient than delivery of DNA in non-dividing cells. *Int J Pharm*. 2010. doi:10.1016/j.ijpharm.2010.01.019

112. Nguyen LT, Atobe K, Barichello JM, Ishida T, Kiwada H. Complex formation with plasmid DNA increases the cytotoxicity of cationic liposomes. *Biol Pharm Bull*. 2007. doi:10.1248/bpb.30.751

113. Dan N. Lipid-nucleic acid supramolecular complexes: Lipoplex structure and the kinetics of formation. *AIMS Biophys*. 2015. doi:10.3934/biophy.2015.2.163

114. Khan S, Soni S, Veerapu NS. HCV Replicon Systems: Workhorses of Drug Discovery and Resistance. *Front Cell Infect Microbiol*. 2020;10(June):1-16. doi:10.3389/fcimb.2020.00325

115. Edelmann FT, Niedner A, Niessing D. Production of pure and functional RNA for in vitro reconstitution experiments. *Methods*. 2014. doi:10.1016/j.ymeth.2013.08.034

116. Gallo S, Furler M, Sigel RKO. In vitro transcription and purification of RNAs of different size. *Chimia (Aarau)*. 2005. doi:10.2533/000942905777675589

117. Marcotrigiano J, Gingras AC, Sonenberg N, Burley SK. Cap-dependent translation initiation in eukaryotes is regulated by a molecular mimic of elF4G. *Mol Cell*. 1999. doi:10.1016/S1097-2765(01)80003-4

118. Mu X, Greenwald E, Ahmad S, Hur S. An origin of the immunogenicity of in vitro transcribed RNA. *Nucleic Acids Res*. 2018. doi:10.1093/nar/gky177

119. Bochkov YA, Palmenberg AC. Translational efficiency of EMCV IRES in bicistronic vectors is dependent upon IRES sequence and gene location. *Biotechniques*. 2006. doi:10.2144/000112243

120. Borman AM, Deliat FG, Kean KM. Sequences within the poliovirus internal ribosome entry segment control viral RNA synthesis. *EMBO J*. 1994. doi:10.1002/j.1460-2075.1994.tb06613.x

121. Kauder SE, Racaniello VR. Poliovirus tropism and attenuation are determined after internal ribosome entry. *J Clin Invest*. 2004. doi:10.1172/JCI200421323

122. Zhao Y, Qin W, Zhang JP, et al. HCV IRES-Mediated Core Expression in Zebrafish. *PLoS One*. 2013. doi:10.1371/journal.pone.0056985

123. Reynolds JE, Kaminski A, Kettinen HJ, et al. Unique features of internal initiation of hepatitis C virus RNA translation. *EMBO J*. 1995. doi:10.1002/j.1460-2075.1995.tb00289.x

124. Gendron K, Ferbeyre G, Heveker N, Brakier-Gingras L. The activity of the HIV-1 IRES is stimulated by oxidative stress and controlled by a negative regulatory element. *Nucleic Acids Res*. 2011. doi:10.1093/nar/gkq885

125. Merrill MK, Dobrikova EY, Gromeier M. Cell-Type-Specific Repression of Internal Ribosome

Entry Site Activity by Double-Stranded RNA-Binding Protein 76. *J Virol*. 2006. doi:10.1128/jvi.80.7.3147-3156.2006

126. Licursi M, Christian SL, Pongnopparat T, Hirasawa K. In vitro and in vivo comparison of viral and cellular internal ribosome entry sites for bicistronic vector expression. *Gene Ther*. 2011. doi:10.1038/gt.2011.11

127. Alvarado-Kristensson M. A simple and fast method for fixation of cultured cell lines that preserves cellular structures containing gamma-tubulin. *MethodsX*. 2018. doi:10.1016/j.mex.2018.02.003

128. Stanly TA, Fritzsche M, Banerji S, et al. Critical importance of appropriate fixation conditions for faithful imaging of receptor microclusters. *Biol Open*. 2016. doi:10.1242/bio.019943

129. WHO. *Global Technical Strategy for Malaria 2016-2030*.; 2015.

7. Annexes

Plasmids and their main transcriptional units

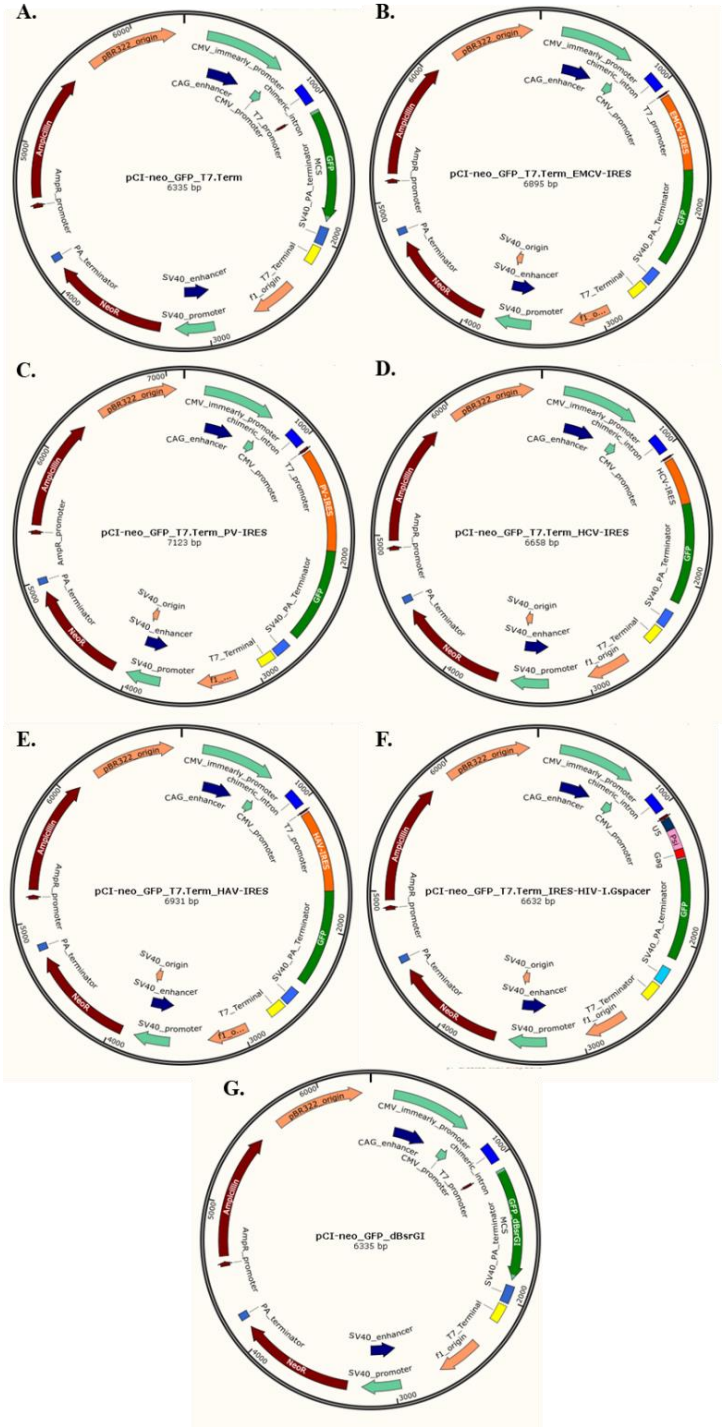

Figure 7.1 - Reporter plasmids used in this work and the respective main transcriptional units. Control plasmid encoding GFP, used for RNA transcription through recognition of T7 promoter and T7 terminator (A); Plasmid derived from A encoding GFP under the IRES regulation from: EMCV (B), PV (C), HCV (D), HAV (E) and HIV-1 (F). Plasmid derived from A encoding the mutated GFP, with the BsrGI restriction site deletion (G).

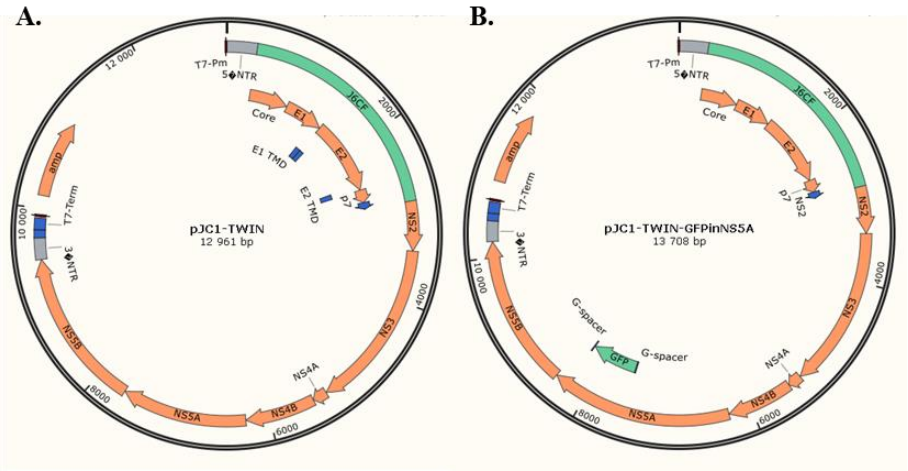

Figure 7.2 - J6/C replicon plasmids used in this work and the respective main transcriptional units. Original plasmid of the full-length J6/C chimeric replicon genome, encoding all HCV proteins (A). New plasmid derived from plasmid A, encoding GFP fused in NS5A, the tagged replicon (B).

Table 7.1 - Primers and templates for plasmid construction

Cloning primers, templates and gBlocks				
Final construct	**Insert**	**Source**	**Cloning vector**	**Primers 5´→ 3´sequence**
pCI-NEO_GFP_T7.Term	GFP	pRRLSIN.hPGK_GFP_WPRE	pCI-NEO	F: CTAGCCTCGAGAATTCGCCACCATGGTGAGCAAGGG R: TACCACGCGTGAATTTTACTTGTACAGCTCGTCCA
	T7 Terminator	T7.Term- gBlocks		N/ A
pCI-NEO_mCherry_T7.Term	mCherry	pPuro_mCherry	pCI-NEO	F: CTAGCCTCGAGAATTCGCCACCATGGTGAGCAAGGG R: TACCACGCGTGAATTCTAGCTTACTTGTACAGCTC
	T7 Terminator	T7.Term- gBlocks		N/ A
pCI-NEO_GFP_T7.Term_IRES-POLI	IRES-POLI	pRLUC__POLIRES_FLUC	pCI-NEO_GFP_T7.Term	F: TCACTATAGGCTAGCAAGCTTGGGCTGCAGGTCTT R: CTAGCCTCGAGAATTATCTTAACAATGAGGTAATT
pCI-NEO_GFP_T7.Term_IRES-EMCV	IRES-EMCV	pMIG	pCI-NEO_GFP_T7.Term	F: TCACTATAGGCTAGCCCCCCCCCCCCTAACGTTAC R: CTAGCCTCGAGAATTCGTGTTTTTCAAAGGAAAAC
pCI-NEO_GFP_T7.Term_IRES-HAV	IRES-HAV	IRES-HAV-gBlocks	pCI-NEO_GFP_T7.Term	N/ A
pCI-NEO_GFP_T7.Term_IRES-HCV	IRES-HCV	pJ6/C	pCI-NEO_GFP_T7.Term	F: TCACTATAGGCTAGCACCTGCCCCTAATAGGGGCG R: CTAGCCTCGAGAATTGGTGCACGGTCTACGAGACC
pCI-NEO_GFP_T7.Term_IRES-RETRO.Gspacer	IRES-RETRO.Gspacer	pRRLSINPPTPGK_GFP_WPRE	pCI-NEO_GFP_T7.Term	F: TCACTATAGGCTAGCAAGTAGTGTGTGCCCGTCTG R: ACCATGCTGCCTCCGCCGCCACCGAATTTTTTCCCATCGC
	GFP.wGspacer	pCI-NEO_GFP_T7.Term		F: GGCGGCGGAGGCAGCATGGTGAGCAAGGGCGAGGA R: AAATGAATGCAATTGGATATAGTTCCTCCTTTCAG

Table 7.2 - Double stranded DNA fragments

gBlocks	T7 Terminal	TTAACAACAACAATTAGGCTGCTAACAAAGCCCGAAAGGAAGCTGAGTTGGCTGCTGCCACCGCTGAGCAATAACT AGCATAACCCCTTGGGGCCTCTAAACGGGTCTTGAGGGGTTTTTTGCTGAAAGGAGGAACTATATCCAATTGCATTC ATTTT
Plasmids	IRES-HAV	CTCACTATAGGCTAGCACCTGCCCCTAATAGGGGCGACACTCCGCCATGAATCACTCCCCTGTGAGGAACTACTGTC TTCACGCAGAAAGCGCCTAGCCATGGCGTTAGTATGAGTGTCGTACAGCCTCCAGGCCCCCCCCTCCCGGGAGAGC CATAGTGGTCTGCGGAACCGGTGAGTACACCGGAATTGCCGGGAAGACTGGGTCCTTTCTTGGATAAACCCACTCTA TGCCCGGCCATTTGGGCGTGCCCCCGCAAGACTGCTAGCCGAGTAGCGTTGGGTTGCGAAAGGCCTTGTGGTACTGC CTGATAGGGCGCTTGCGAGTGCCCCGGGAGGTCTCGTAGACCGTGCACCAATTCTCGAGGCTAG
	GFP- G spacers in NS5A	GTCCGACGTCCCCTGGTGAGCCGGCCCCCTCAGAGACAGGTTCCGCCTCCTCTATGCCCGGCGGCGGAGGCAGCAT GGTGAGCAAGGGCGAGGAGCTGTTCACCGGGGTGGTGCCCATCCTGGTCGAGCTGGACGGCGACGTAAACGGCCAC AAGTTCAGCGTGTCCGGCGAGGGCGAGGGCGATGCCACCTACGGCAAGCTGACCCTGAAGTTCATCTGCACCACCG GCAAGCTGCCCGTGCCCTGGCCCACCCTCGTGACCACCCTGACCTACGGCGTGCAGTGCTTCAGCCGCTACCCCGAC CACATGAAGCAGCACGACTTCTTCAAGTCCGCCATGCCCGAAGGCTACGTCCAGGAGCGCACCATCTTCTTCAAGG ACGACGGCAACTACAAGACCCGCGCCGAGGTGAAGTTCGAGGGCGACACCCTGGTGAACCGCATCGAGCTGAAGG GCATCGACTTCAAGGAGGACGGCAACATCCTGGGGCACAAGCTGGAGTACAACTACAACAGCCACAACGTCTATAT CATGGCCGACAAGCAGAAGAACGGCATCAAGGTGAACTTCAAGATCCGCCACAACATCGAGGACGGCAGCGTGCA GCTCGCCGACCACTACCAGCAGAACACCCCCATCGGCGACGGCCCCGTGCTGCTGCCCGACAACCACTACCTGAGC ACCCAGTCCGCCCTGAGCAAAGACCCCAACGAGAAGCGCGATCACATGGTCCTGCTGGAGTTCGTGACCGCCGCCG GGATCACTCTCGGCATGGACGAGCTGTATAAGGGCGGCGGAGGCAGCCCCCTCGAGGGGGAGCCTGGAGATCCGG ACCTGGAGTCTGATCAGGTAGAGCTTCAACCTCCCCCCCAGGGGGGGGGGGTAGCTCCCGGTTCGGGCTCGGGGTC TTGGTCTACTTGCTCCGAGGAGGACGATACCACCGTGTGCTGCTCCATGTCATACTCCTGGACCGGGGCTCTAATAA CTCCCTGTAGCCCCGAAGAGGAAAAGTTGCCAATCAACCCTTTGAGTAACTCGCTGTTGCGATACCATAACAAGGTG TACT

Primers and probes used for RT-qPCR

Table 7.3 - Primers used for RT-qPCR.

GENE	SEQUENCE
GFP	pF: CAGAAGAACGGCATCAAGGT pR: CTGGGTGCTCAGGTAGTGG
RPL22	pF: CTGCCAATTTTGAGCAGTTT pR: CTTTGCTGTTAGCAACTACGC